

# Preparation and evaluation of metoprolol tartrate patches containing different polymer components

Ph.D. thesis

**József Papp**

Semmelweis University  
Doctoral School of Pharmaceutical Sciences



Supervisor: Dr. Sylvia Marton, Ph.D.

Consulent: Dr. Romána Zelkó, D.Sc.

Reviewers: Dr. Judit Balogh, Ph.D.

Dr. Miklós Vecsernyés, Ph.D.

President of the Theoretical Exam Committee:

Dr. György Bagdy, D.Sc.

Members of the Theoretical Exam Committee:

Dr. Kornélia Tekes, Ph.D.

Dr. Erzsébet Csányi, Ph.D.

Budapest  
2012

# CONTENT

<b>1.</b>	<b>ABBREVIATIONS</b> .....	<b>4</b>
<b>2.</b>	<b>INTRODUCTION</b> .....	<b>6</b>
<b>3.</b>	<b>LITERATURE REVIEW</b> .....	<b>8</b>
<b>3.1.</b>	<b>Therapeutic Systems</b> .....	<b>8</b>
<b>3.2.</b>	<b>Transdermal Therapeutic Systems</b> .....	<b>9</b>
<b>3.3.</b>	<b>Skin as a barrier and transfer to systemic blood circulation</b> .....	<b>10</b>
<b>3.4.</b>	<b>Physicochemical properties of drugs with skin permeation</b> .....	<b>13</b>
<b>3.5.</b>	<b>Enhancing the permeation into the skin</b> .....	<b>14</b>
<b>3.5.1.</b>	<b>Application of physical activation</b> .....	<b>15</b>
3.5.1.1.	Iontophoresis .....	15
3.5.1.2.	Electroporation .....	16
3.5.1.3.	Phonophoresis .....	16
3.5.1.4.	Thermoresponsive systems .....	16
<b>3.5.2.</b>	<b>Application of prodrugs</b> .....	<b>17</b>
<b>3.5.3.</b>	<b>Application of enhancers</b> .....	<b>17</b>
<b>3.6.</b>	<b>Classification of TTS</b> .....	<b>19</b>
<b>3.6.1.</b>	<b>Membrane permeation controlled TTS</b> .....	<b>19</b>
<b>3.6.2.</b>	<b>Adhesive dispersion controlled TTS</b> .....	<b>20</b>
<b>3.6.3.</b>	<b>Matrix diffusion controlled TTS</b> .....	<b>21</b>
<b>3.6.4.</b>	<b>Microreservoir controlled TTS</b> .....	<b>22</b>
<b>3.7.</b>	<b>Kinetic consideration of TTS</b> .....	<b>23</b>
<b>3.7.1.</b>	<b>Release kinetics from matrix devices</b> .....	<b>24</b>
<b>3.7.2.</b>	<b>Release kinetics from gelled liquid reservoir systems</b> .....	<b>26</b>
<b>3.7.3.</b>	<b>Analysis of the release profiles according to different kinetic models</b> .....	<b>26</b>
<b>4.</b>	<b>OBJECTIVES</b> .....	<b>28</b>
<b>5.</b>	<b>EXPERIMENTAL PART</b> .....	<b>29</b>
<b>5.1.</b>	<b>Materials and methods</b> .....	<b>29</b>

<b>5.1.1. Materials</b> .....	<b>29</b>
5.1.1.1. Application of metoprolol tartrate.....	29
5.1.1.2. Application of acrylates.....	31
5.1.1.3. Application of cellulose ether polymers.....	32
5.1.1.3.1. Methylcellulose.....	32
5.1.1.3.2. Hypromellose.....	34
<b>5.1.2. Methods</b> .....	<b>36</b>
5.1.2.1. Method for preparation of patches.....	36
5.1.2.2. Organoleptic examination of different compositions for preparing applicable patches.....	36
5.1.2.3. Viscosity measurements.....	36
5.1.2.4. Optimization of composition according to the drug liberation examinations.....	37
5.1.2.5. Analysis of the release profiles according to different kinetic models.....	38
5.1.2.6. FT-IR examinations.....	38
5.1.2.7. Non-invasive stability screening of patches with ATR-FTIR examinations.....	38
5.1.2.8. Positron annihilation lifetime spectroscopy (PALS).....	38
<b>5.2. Results</b> .....	<b>41</b>
<b>5.2.1. Preformulation examinations</b> .....	<b>41</b>
5.2.1.1. Preparation of Eudragit films for further formulation of matrices containing metoprolol tartrate.....	41
5.2.1.2. Optimization of formulations using different Metolose types.....	43
5.2.1.3. Viscosity aspects for the preformulations.....	44
<b>5.2.2. Results of the analysis of the TTS systems</b> .....	<b>45</b>
5.2.2.1. Drug liberation examinations.....	45
5.2.2.2. Storage of patches.....	47
5.2.2.3. FT-IR examinations.....	49
5.2.2.4. Positron annihilation lifetime spectroscopy (PALS).....	52
<b>5.3. Discussions</b> .....	<b>53</b>
<b>5.3.1. Formulation considerations of applicable patches</b> .....	<b>53</b>
<b>5.3.2. Kinetic considerations of the release profiles</b> .....	<b>54</b>

<b>5.3.3. Non-invasive stability screening of patches</b> .....	<b>55</b>
<b>5.3.4. Relationship between FT-IR spectra and kinetic data of patches</b> .....	<b>55</b>
<b>5.3.5. Aspects of the positron annihilation lifetime spectroscopy (PALS) results</b> .....	<b>57</b>
<b>6. NEW SCIENTIFIC RESULTS AND CONCLUSIONS</b> .....	<b>61</b>
<b>7. SUMMARY</b> .....	<b>63</b>
<b>8. ÖSSZEFOGLALÓ</b> .....	<b>64</b>
<b>9. REFERENCES</b> .....	<b>65</b>
<b>10. PUBLICATIONS AND LECTURES</b> .....	<b>79</b>
<b>11. ACKNOWLEDGEMENTS</b> .....	<b>80</b>

# 1. ABBREVIATIONS

A	~ cross-sectional area
$A_i$	~ initial drug concentration
$A_i$	~ relative intensities
ATR-FTIR	~ Attenuated total reflectance Fourier transform infrared spectroscopy
AUC	~ area under curve
$C_s$	~ saturation solubility
CNS	~ central nervous system
D	~ diffusion coefficient
Da	~ Dalton
dC	~ concentration gradient
dt	~ time of diffusion
dx	~ thickness of a layer
dw	~ quantity of the dissolved substance
F	~ fraction released from matrix devices
FT-IR	~ Fourier transform infrared spectroscopy
G	~ rotation speed
h	~ hour
$h(\lambda)$	~ lifetime distribution function
<i>iv</i>	~ intravenous
JPE	~ Japanese Pharmaceutical Excipients
k	~ rate constant of the drug release
L	~ thickness of matrix film
$M_t$	~ amount of the drug released at time t
$M_\infty$	~ total amount of the released drug at infinite time
n	~ number of samples
o-Ps	~ ortho-positronium atom
PALS	~ positron annihilation lifetime spectroscopy
PSA	~ pressure sensitive adhesives
Ph. Eur.	~ European Pharmacopoeia
Ps	~ positronium
R	~ radius of the free volume hole
$R^2$	~ correlation coefficient
RSD	~ relative standard deviation
$S(t)$	~ lifetime spectrum
$t_0$	~ lag-time (min) of the dissolution
TTS	~ transdermal therapeutic system
USP/NF	~ United States Pharmacopeia – National Formulary
% w/w	~ percentage weight in weight
$\lambda_I$	~ separate lifetimes
$\beta$	~ shape parameter of the curve
$\Delta R$	~ constant for the positronium lifetime
$\varepsilon$	~ porosity
T	~ tortuosity
$\tau_{63.2}$	~ time (min) when 63.2% of $M_\infty$ has been dissolved

$\tau$  ~ positronium lifetime  
 $\tau_2$  ~ medium long lifetime  
 $\tau_3$  ~ positron lifetime spectra

## 2. INTRODUCTION

Transdermal therapeutic systems (TTSs) allow delivery of contained drug into the systemic circulation via permeation through skin layers at a controlled rate. These systems are easy to apply and remove as and when desired. This approach of drug delivery is more pertinent in case of chronic disorders, such as hypertension, which require long-term dosing to maintain therapeutic drug concentration. Transdermal delivery of cardiovascular drugs offers several advantages, and transdermal forms of nitroglycerin and clonidine have been marketed. Transdermal delivery of one of the common class of cardiovascular drugs,  $\beta$ -blockers, has also been investigated and can offer benefits. Metoprolol tartrate is a selective hydrophilic  $\beta$ -blocking agent for the treatment of mild and moderate hypertension and also for long term management of angina pectoris. Metoprolol tartrate with hydrophilic character is 95% absorbed and has a bioavailability of 40- to 50% in oral dosage forms. Peak plasma concentrations are achieved after 2–3 hours, and half life of the molecule is 3 to 7 hours. This makes frequent dosing necessary to maintain the therapeutic blood levels of the drug for long-term treatment. The n-octanol/water partition coefficient is 0.98 at pH 7.4. Therefore, metoprolol is an ideal drug candidate for transdermal drug delivery, which makes a once-a-day dose treatment possible, thus improving the patient compliance.

Matrix type TTS could be an appropriate vehicle for sustain-release of metoprolol tartrate. The application of different polymer matrices enables the control of the rate and the amount of the released drug. Acrylic polymers (Eudragit) and cellulose ether polymers (Metolose) are often used in pharmaceutical preparations with different purposes, such as binding-, coating- and sealing tablets, and also for retarding the drug release from tablets. Acrylic polymers have good skin compatibility, and are able to form films. Metolose polymers can also be characterized with good skin compatibility and film forming ability. Applying the casting method they can be ideally combined with each other for film forming. Choose of different types of these excipients enables the influence of the drug release rate- and amount from the vehicles containing metoprolol tartrate.

In order to reveal information about the structure of polymer films containing drugs are mainly NMR, X-ray diffraction and thermoanalytical methods applied. The use of

atomic force microscopy makes possible to get much more detailed information about their 3D surface properties. A new promising method for the analysis of polymer films is the application of positron annihilation lifetime spectroscopy (PALS), which gives valuable data about the supramolecular characteristics of patches with the determination of the sizes and distributions of free volume holes of polymers.



### **3. LITERATURE REVIEW**

#### ***3.1. THERAPEUTIC SYSTEMS***

The classical dosage forms are usually 2 dimensional including dose in volume. The next generations of drug products are 3 dimensional forms, where the third dimension is time.

The 3 dimensional preparations include:

- prolonged action preparations
- controlled release dosage forms
- targeted delivery systems
- pulsatile release.

Among these categories the controlled release dosage forms contain the therapeutic systems. The most popular representatives of this class are the transdermal therapeutic systems (TTS).

The applied drug can be given by the use of therapeutic systems during a predetermined time with steady-state delivery rate. These systems do not always contain the usual (oral) dosage, which can lower the onset of side-effects. They are also able to sustain constant therapeutic steady-state blood level, because the eliminated drug is supplied by these systems to the body and / or to the determined organ.

With the recognition of the advantages of these systems, they are widely used in therapies of several diseases.

They can be categorized as follows [1]:

- I. Therapeutic systems with systemic effect
  - parenteral systems
  - transdermal therapeutic systems
  - oral therapeutic systems
    - oral osmotic therapeutic systems

- pulsating therapeutic system
- rectal therapeutic systems

II. Therapeutic systems with local effect

- therapeutic systems for intrauterine application
- ophthalmic therapeutic systems.

### **3.2. *TRANSDERMAL THERAPEUTIC SYSTEMS***

The drug content of transdermal therapeutic systems (TTS) is able to penetrate through the different layers of the skin to reach the systemic circulation and / or the organ, where the drug is ready to give its therapeutic effect.

There are many advantages of these systems [2-5]:

- the drug avoids the liver, which results in delayed metabolization of the drug
- it does not oppress the liver and the GI tract
- it enhances the biological half time of the drug (through avoiding the liver)
- it results in higher bioavailability of the drug
- toxicity and side effects are lowered
- it enables an application form without pain
- they ensure precise dosage
- smaller doses can also give the same therapeutic effect
- there can be also drugs applied, which could be used only via *iv.* injection or infusion because of the metabolization
- they lower the risk of microbiological contamination
- the effect of food and drinks does not affect the liberation of the drug
- drugs with short biological half time can be also applied
- enhance the patient compliance
- the eventually negative effect of the drug can be terminated with the removal of the patches.

Most of the dermal preparations are creams and ointments, which do not enable precise dosage of the drug, because the thickness of the applied preparation cannot be exactly determined, and it is fast unavoidable to wash off some part of the system [6]. To reach the required local therapeutic effect they need to be applied not only once a day.

These clinical facts lead to the development of the transdermal therapeutic systems (TTS), which are able to ensure systemic effect with predetermined time with steady-state delivery rate.

There are also disadvantages of TTS [7-10]:

- at the first time of application, a certain time is needed to reach the therapeutic blood level
- drugs, the application of which led to skin irritation are not applicable in TTS
- chemical modifiers in patches can also lead to skin irritation
- extended application at the same surface of the skin can cause allergy symptoms
- a limited range of drugs can be applied in TTS because of the slight penetration into the skin structure.

### ***3.3. SKIN AS A BARRIER AND TRANSFER TO SYSTEMIC BLOOD CIRCULATION***

Skin, as the biggest organ, plays a very important role in the protection of the body through chemical- and physical protection. The three main layers of the skin are:

- epidermis
- dermis
- subcutis.

The main barriers to transdermal delivery are the stratum corneum and the stratum lucidum in the epidermis layer, respectively. The stratum corneum is a horny layer of the skin; the thickness of this layer is between 10 -15  $\mu\text{m}$  and consists of 10-25 layers. It is a parallel array of thin plates, which are stratified on each other and consist of mainly

proteins [11, 12]. There can be found intercellular lamellar lipids between these thin layers. They are residue of the membrane surrounding each epidermal cell and they come into existence when the epidermal cells are embodied. This lipid contains ceramides, free sterols, free acids, sterol esters, triglycerides, etc. These lipids are able to organize themselves into membrane bilayers, although they do not contain any phospholipids [13]. All the components of the interstitial lipids contribute to the barrier function of the stratum corneum. Figure 1 illustrates the different layers of the skin.

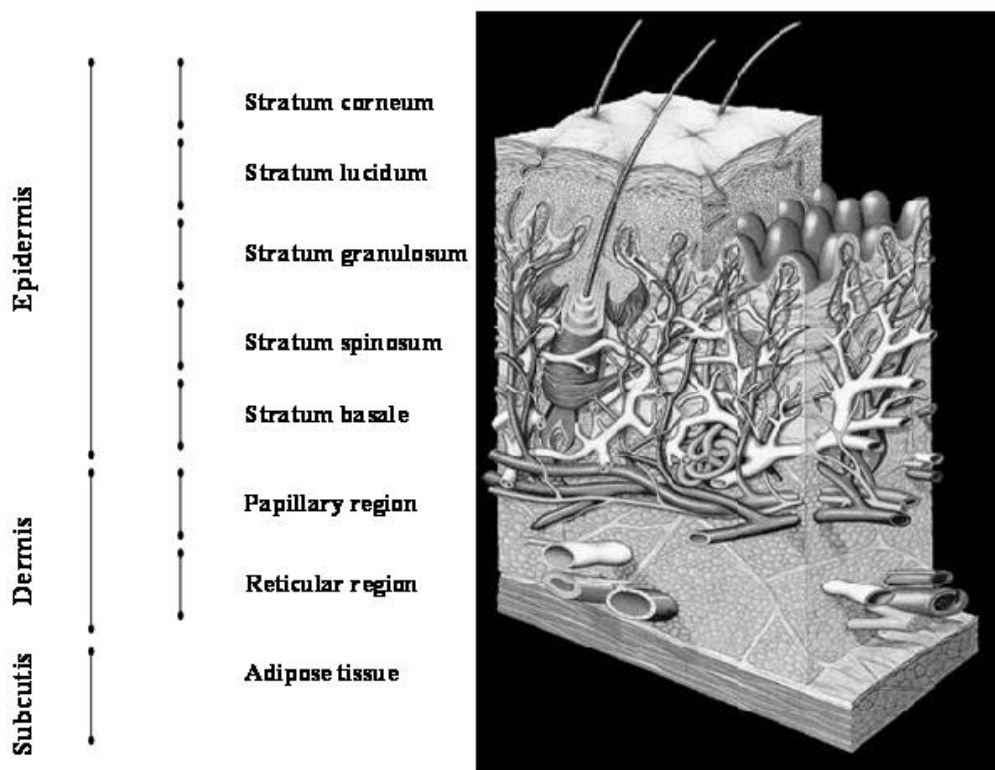


**Figure 1** – The different layers of the skin [14]

The transepidermal delivery of the drugs has three major pathways in the stratum corneum [15, 16]

- paracellular
- transcellular
- appendageal.

The paracellular pathway involves the lamellar lipids into the transport of drugs, which are essentially responsible for the sticking of the epidermal cells. During the transcellular transportation the drugs pass through the cells of the stratum corneum. Most of the substances diffuse through this layer via the paracellular lipoidal pathway [17]. Nonetheless, paracellular and transcellular routes can play a role in combination during the transportation of drugs. The appendage route composed of hair follicles, sebaceous glands and sweat glands is considered to be substantially less important for drug transport, as this route accounts for less than 0.1 percent of the total surface area of the skin. This route may be of some importance for large ionic molecules. Drugs which diffuse through the sebaceous glands come first into the dermis and then into the subcutis [18, 19]. Figure 2 shows the routes of transdermal delivery.

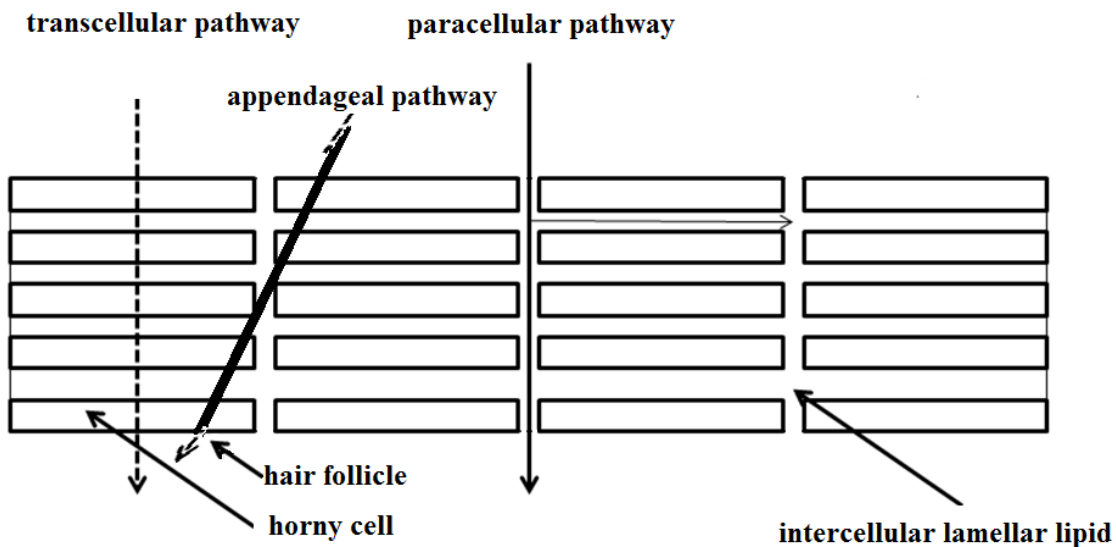


**Figure 2** – Delivery pathways of transdermal delivery

The other important barrier for many drugs is the stratum lucidum, which consist of 1 or 2 cell lines. It is an electronegative barrier and the electronegative drugs are not able to cross the stratum lucidum because of this negative shift. The positively charged drugs are pulled by this layer. Iontophoretic treatment can extinguish the effect of this barrier [20, 21]. The drugs can pass through the dermis and the subcutis easier.

At the surface of the skin there can be found an acid protecting layer, through which all the hydrophilic and also the hydrophobic drugs need to pass [22].

### **3.4. *PHYSICOCHEMICAL PROPERTIES OF DRUGS WITH SKIN PERMEATION***

The lipids in the epidermis play a very important role in the penetration of drugs into the skin. The protein parts of the epidermis can bind water and they become hydrated. This hydrated state helps also in the better penetration of drugs. With this hydration the dermis behaves as a protein gel regarding the penetration of the drugs. Whether the drug can penetrate into the skin and reach the systemic blood circulation and / or the specific organ depends also on the structure of the drug. Most drugs are not suitable for transdermal delivery for one or more reasons. The desirable physicochemical, pharmacokinetic and biopharmaceutical characteristics of a candidate drug are:

- low daily dose (less than 20 mg/day)
- short half-life (10 hours or less)
- low molecular weight (less than 400 Da)
- low melting point (less than 200°C)
- high lipid solubility (octanol/water partition coefficient – /logP/ between -1.0 and 4)
- high skin permeability (permeability coefficient greater than  $0.5 \times 10^{-3}$  cm/h)
- non-irritating and non-sensitizing to skin.

Low oral bioavailability and low therapeutic index, which requires tight control of plasma levels, are not required characteristics of drugs for transdermal delivery, but they confirm the application of a candidate drug in TTS [23- 28].

Generally only a few of the candidates could fulfill all these requirements: the high oral daily dose, large patch size, skin irritation or sensitization forms the main barriers for

the transdermal application. An acceptable balance between these requirements must be established for the drug delivery in TTS.

Drugs can have high skin permeability with the following characteristics:

- high dipole moments
- able to form hydrogen binding
- are amphiphilic
- have low molecular weight.

If the drugs are applied on the skin they can

- treat local diseases or
- they can form reservoirs glued to the cells of the stratum corneum or of the dermis or
- they can penetrate into the deeper regions of the skin or
- they are metabolized by the enzymes of the skin or
- they can penetrate into the microcirculatory system.

### ***3.5. ENHANCING THE PERMEATION INTO THE SKIN***

Transdermal systems are applied in not such a wide range in the practice because of the poor permeation of the drugs into the skin. There are several possibilities to improve the permeation of drugs into the skin:

Physical methods

- scraping of the stratum corneum
- hydration of the stratum corneum [29, 30]
- iontophoresis [31]
- electroporation

- application of ultrasound energy on the skin
- application of thermal energy.

Chemical methods:

- synthesis of lipophilic drugs
- delipidation of the stratum corneum
- application of enhancers to help the penetration of drugs into the skin [32-34].

Biochemical methods:

- synthesis of prodrugs which are able for bioconversion in the skin [35, 36]
- application of enhancers can reduce the residence time in the skin, and thus decrease the cutaneous metabolism of drugs.

### 3.5.1. Application of physical activation

#### 3.5.1.1. *Iontophoresis*

Iontophoresis involves application of a low intensity electric current to facilitate the permeation of a drug into the skin. Iontophoresis can increase the rate of transdermal penetration of hydrophilic compounds [37, 38].

Peptides could not be applied in TTS because of their high molecular weight, instability, low biological half-life and mainly polar characteristics [39]. The application of iontophoresis helps to transport protein molecules into the skin (transport of insulin) [40].



### 3.5.1.2. *Electroporation*

Electroporation is a method of application of short, high voltage electrical pulses to the skin. These electrical pulses form transient aqueous pores in the stratum corneum through which the drug molecules pass with electrophoresis and / or electroosmosis. This method allows a much more effective diffusion of drugs, respectively in the case of proteins [41-43]. The disadvantage of this system is the nerve irritation caused by the application of electrical pulses. The application of 2 phase continuous current can minimize the irritation and the lesion of the nerve endings. Electroporation can be achieved also with patches of which structure is much more difficult and therefore the production is more expensive.

### 3.5.1.3. *Phonophoresis*

Phonophoresis (or sonophoresis) uses ultrasound energy in order to enhance the skin penetration of active substances [44-46]. When skin is exposed to ultrasound, the waves propagate to a certain level and cause several effects that assist skin penetration. One of these effects is the cavitation, which means formation and subsequent collapse of gas bubbles in a liquid. This cavitation leads to formation of holes in the corneocytes, enlargement of intercellular spaces, and perturbation of stratum corneum lipids. Another effect is the heating of skin due to the energy loss of the propagating ultrasound wave (scattering and absorption effects). The resulting temperature elevation will increase the fluidity of the stratum corneum lipids and increase the diffusivity of molecules through the skin barrier. These main effects can be assisted by acoustic microstreaming caused by the acoustic shear stress which is due to unequal distribution of pressure forces.

### 3.5.1.4. *Thermoresponsive systems*

A new direction for pharmaceutical and medical research have been made with formulations based on stimuli-responsive polymers, because temporal drug release may be required, when the severity of disease symptoms fluctuate with time. If discontinuous changes in drug release rates are required in response to a small change

of temperature, thermoresponsive polymers may be used to develop hydrogels which react with their physical characteristics on the changes of their environment [47-49].

Thermoresponsive transdermal therapeutic systems consist of thermoresponsive agents (polymer, liquid crystals, liposomes), which suffer phase transition according to the change of temperature regulating drug delivery. This phase transition may be soluble-insoluble state variation, sol-gel transition, liquid crystal phase transitions, crystalline-amorphous phase-oscillation [50-52], etc.

### 3.5.2. Application of prodrugs

Prodrugs are inactive forms of drugs, which are transferred in the body with hydrolytic and enzymatic bioconversion into the active forms of drugs. The application of prodrugs has an important role in the case of drugs, which could not penetrate in the original form into the skin [53, 54].

At the application of TTS the drugs pass the different layers of the skin, where they can be modified by the metabolic enzymes (such as o-methyltransferase, aryl-hydrocarbon-hydrolase) [55]. The inactive prodrugs are metabolized with these enzymes into the active drugs. This bioconversion can be applied for example in the case of the less permeable estrogen. These esterificated estrogens (estradiol acetate, estradiol diacetate, estradiol valerate) can penetrate into the skin much more intensively and they are fast metabolized by the esterase enzyme in the skin and form the active estradiol [56-58].

### 3.5.3. Application of enhancers

Increasing drug penetration through the skin needs penetration enhancers which modify the lipid organization in the stratum corneum. Depending on their molecular structure they can act in the following ways:

- intercalating into the sublattice, which leads to the modification of the sublattice

- disturbing of the lamellar packing
- forming separate small domains in the lateral packing in the lamellae
- forming enhancer-rich large separate domains in the intercellular regions [59, 60].

The structure of skin is modified as a result at the application of enhancers:

- they can change the hydration of the skin thanks to their higher water content in comparison with the skin. In this case the evaporation of the water in the TTS can lead to the hydration of the skin.
- lipophilic enhancers form a thin layer on the surface of the skin and lower the evaporation of the endogenous water from the skin (W/O emulsions) [61].

The transepidermal transportation of drugs can be positively affected by the hydration of the different layers of the skin. The transfollicular pathway can lead to a problem that the drug and the enhancer can be separated from each other in the sebaceous glands.

The keratolytic agents can loosen up the structure of the stratum corneum.

The surface active ingredients can solubilize the fat layer, which can quicken the transport during the lipid layer. These enhancers can be saturated and unsaturated fatty acids, from which the dodecyl chain length or the unsaturated C18 chain length is the most favorable for increasing drug transport across the skin [62, 63]. The fatty acids are applied with hydrocortisone or indomethacin [64, 65].

There are also other enhancers such as dimethyl sulfoxide [66, 67].

There is no general preference for any particular penetration enhancer or family of enhancers, because their effect depends on the interactions with the applied drug. The different types of enhancers can be varied with each other to goal a better absorption into the skin.

### **3.6. CLASSIFICATION OF TTS**

In the general characterization of TTS are the following components:

- backing films
- drug reservoir
- rate-controlling membrane
- pressure sensitive adhesives (PSA)
- protective pressure sensitive adhesive release liner.

In many cases one component can fulfill the role of the other components.

The TTSs can be classified on the base of the drug-release mechanism:

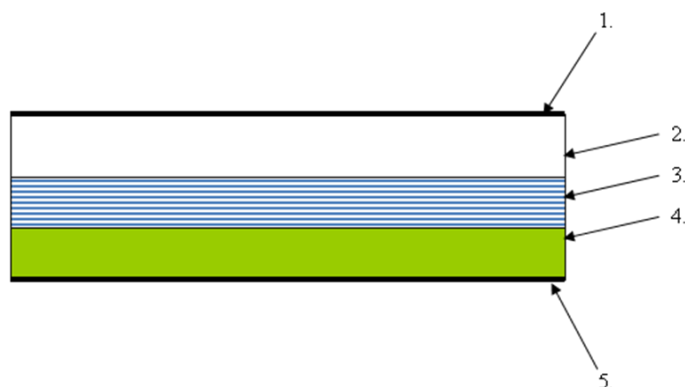
- membrane permeation controlled patch
- adhesive dispersion controlled patch
- matrix diffusion controlled patch
- microreservoir controlled patch.

The TTSs are characterized by steady-state delivery rate, the whole dose and the complete area of drug release.

#### **3.6.1. Membrane permeation controlled TTS**

The release-rate from the reservoir is controlled by a membrane which is permeable for the drug. This membrane can be porous or not porous polymer membrane. The outer surface of the membrane is thin, compatible with the drug and hypoallergenic. The pressure sensitive adhesive ensures the cohesion between the skin and the TTS (Figure 3). The release-rate of the drug is influenced by the structure and the composition of the

reservoir, by the composition of the rate-controlling membrane and by the thickness, the structure and the permeability coefficient of the adhesive.



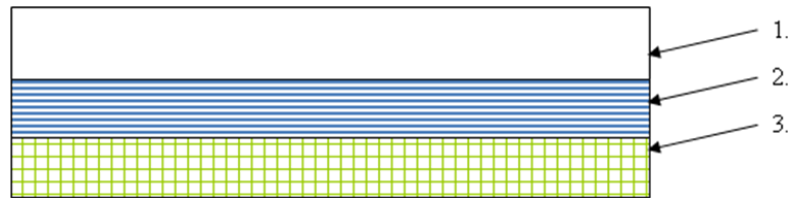
1. impermeable backing liner; 2. drug reservoir; 3. rate-controlling membrane;  
4. pressure sensitive adhesive; 5. release liner

**Figure 3** – Structure of membrane permeation controlled patch

The main advantage of this TTS is the nearly constant drug release-rate and the disadvantage is the intensive growth of drug release (dose dumping), if the membrane is damaged [68-70].

### 3.6.2. Adhesive dispersion controlled TTS

In this simplified membrane permeation controlled patch the drug enhancer adhesive matrix polymer contains the drug (it is dispersed in polyisobutylene, polyacrylate polymers). This polymer matrix is clamped to the impermeable backing liner in one or more layers [71, 72]. The disadvantage of this type of TTS is that the drug release-rate is getting smaller during the time of application because of the expansion of the polymer layer (the drug needs to diffuse through this layer). This release-rate can be enhanced with the application of more polymer layers, which have more drug content [73]. Figure 4 illustrates the structure of adhesive dispersion controlled patches.



1. impermeable backing layer; 2. drug in adhesive; 3. release liner

**Figure 4** – Structure of adhesive dispersion controlled patch

### 3.6.3. Matrix diffusion controlled TTS

The matrix diffusion controlled patches (Figure 5) have more simple structure in comparison with the other type of TTS's: they do not contain any rate-controlling membrane [74, 75].



1. impermeable backing layer; 2. absorbent pad; 3. occlusive baseplate;  
4. drug reservoir; 5. adhesive; 6. release liner

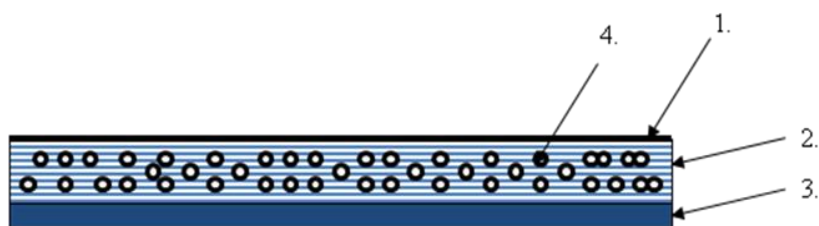
**Figure 5** – Matrix diffusion controlled patch

Drug reservoir is prepared by dissolving the drug and polymer in a common water-based solvent. The insoluble drug should be homogeneously dispersed in hydrophilic or

lipophilic polymer. The required quantity of plasticizer (triethylcitrate, polyethylene glycol, propylene glycol and permeation enhancer) is then added and mixed properly. The medicated polymer is then moulded into rings with defined surface area and controlled thickness over the teflon cover on horizontal surface followed by solvent evaporation at an elevated temperature. The formed film is then separated from the rings, which is then mounted onto an occlusive base plate in a compartment fabricated from a drug impermeable backing. Adhesive polymer is then spread along the circumference of the film [76]. Commonly used polymers for matrix are cross linked polyethylene glycol, polyacrylates, ethylcellulose, polyvinylpyrrolidone and hydroxypropyl methylcellulose. In an ideal case, the swelling of the polymer, which contains the drug, can be influenced that way, that the fluxation of water into the polymer and the diffusion of the drug occur at steady-state rate. Advantages of matrix patches include absence of dose dumping, direct exposure of polymeric matrix to the skin and no interference of adhesive.

#### 3.6.4. Microreservoir controlled TTS

The drug is suspended in an aqueous solution of water miscible drug solubilizer e.g. polyethylene glycol. The drug suspension is homogenously dispersed by a high shear mechanical force in lipophilic polymer, forming thousands of microscopic drug reservoirs (10-200  $\mu\text{m}$ ). The dispersion is quickly stabilized by cross-linking the polymer chains in-situ, which produces a medicated polymer disc of a specific area and fixed thickness. Occlusive base plate mounted between the medicated disc and adhesive form backing prevent the loss of drug through the backing membrane [77]. This system is exemplified by development of Nitrodisc<sup>®</sup>. Figure 6 presents the structure of microreservoir controlled patch.



1. impermeable backing layer; 2. drug in adhesive; 3. release liner  
4. drug reservoir

**Figure 6** – Microreservoir controlled patch

### 3.7. *KINETIC CONSIDERATION OF TTS*

Based on observations of experimental data, it may be stated that the differences in the therapeutic effect of different drug products (which contain the same drug constituents) are most frequently caused by differences in the rates at which the active ingredients are liberated from the given dosage form [78].

The process of diffusion has been described quantitatively by Fick, who adapted equations of thermal conductivity applied earlier by Fourier to diffusion. The definition of the law is as follows: the quantity of the dissolved substance ( $dw$ ) which diffuses at a constant temperature through a cross-sectional area ( $A$ ) within a time ( $dt$ ), through a layer of thickness ( $dx$ ) which is perpendicular to surface  $A$  on the effect of a concentration gradient ( $dC$ ):

$$\frac{dw}{dt} = -DA \frac{dC}{dx} \quad (1)$$

where  $D$  is the diffusion coefficient (the quantity of dissolved substance which diffuses through a  $1 \text{ cm}^2$  cross-sectional area per unit time).



For the characterization of different dosage forms are applied different kinetic models, which are based on the equation of Fick.

The TTS can be grouped in 2 major types respectively the release kinetics of drugs:

- adhesive matrix systems
- gelled liquid reservoir systems.

### 3.7.1. Release kinetics from matrix devices

In dissolved systems, an adhesive matrix system contains drug dissolved at or below the saturation solubility of the drug in the adhesive. Diffusion of drug occurs from the surface of patch into water or skin. In ideal case, the fraction (F) released from a matrix system is described as follows [79]:

$$F = \frac{M_t}{M_\infty} = 1 - 8 \exp \left[ \frac{-D(2n+1)^2 \pi^2 t}{4L^2} \right] \quad (2)$$

where:

$M_t$ = amount of drug released into a sink at time t

$M_\infty$ = amount released on depletion of the device

D= diffusion coefficient

L= thickness of matrix film

n= integer

This equation (2) is more complex in nature, so for simplicity it can be distinguished an early-time and a late portion and they can characterized with different equations [80, 81].

The drug can be found in dispersed-type systems as finely divided particles uniformly dispersed in the polymer matrix. Therefore, the initial drug concentration ( $A_i$ ) is greater than the saturation solubility ( $C_s$ ). The drug release kinetics from a dispersed-type matrix system is described as follows [82]:

$$F = \frac{2}{A_i L} \left[ D C_s (2A_i - C_s) t \right]^{0,5} \quad (3)$$

where:

$C_s$ = saturation solubility

$A_i$ = initial drug concentration

Once the dispersed drug is exhausted from the matrix, the drug release kinetics essentially follows the kinetics of drugs from dissolved systems.

The porous matrix system has continuous macroscopic channels. The release kinetics is mainly dependent on the transport of drug through these tortuous channels. The following equation (4) describes the release kinetics of a drug from these porous matrix systems [83]:

$$M_t = \left[ \frac{D \varepsilon}{T(2A - \varepsilon C_s) C_s t} \right]^{0,5} \quad (4)$$

where:

$\varepsilon$ = porosity

$T$ = tortuosity

The porosity can be determined from the volume fraction of the transdermal device that is permeated by solvent. Tortuosity is a measure of the diffusion length, which the solute would traverse through the channel in excess of linear path [84, 85].

In the absence of porosity and tortuosity in the matrix device, equations 3 and 4 are the same.

### 3.7.2. Release kinetics from gelled liquid reservoir systems

Reservoir patches contain the drug mainly in solution in appropriate vesicles. The viscosity of this solution is increased with an appropriate gelling or thickening agent to make the fabrication of the reservoir patches easier. The release kinetics of the drug through the gel and the rate-controlling membrane of a liquid reservoir patch follow Fick's law of diffusion.

### 3.7.3. Analysis of the release profiles according to different kinetic models

In the *in vitro* evaluation of patches are often applied the following models, which are more simplified as the ones described above and are often used in the kinetic characterization of transdermal devices.

#### *Zero-order model*

The drug release from the dosage form follows a steady-state release running at a constant rate [86, 87]:

$$M_t/M_\infty = kt \quad (5)$$

where

$M_t$  = the amount of the drug released at time  $t$ ,

$M_\infty$  = the total amount of the released drug at infinite time,

$k$  = the zero order rate constant of the drug release.

This model can be applied for drug dissolution from pharmaceutical dosage forms that do not disaggregate and release the drug slowly (assuming that area does not change and no equilibrium conditions are obtained).

*First-order model*

The drug activity within the reservoir is assumed to decline exponentially and the release rate is proportional to the residual activity:

$$M_t/M_\infty = 1 - \exp(-kt) \quad (6)$$

where

k= first order rate constant of the drug release.

*Weibull model*

A general empirical equation described by Weibull was adapted to the dissolution / release process. This equation can be successfully applied to almost all kinds of dissolution curves and is commonly used in kinetic studies.

To characterize the dissolution profile of patches the Weibull distribution was applied in the following form [88]:

$$M_t = M_\infty \left[ 1 - \exp - \left( \frac{t - t_0}{\tau_{63.2}} \right)^\beta \right] \quad (7)$$

where

$M_t$ =the dissolution (%) at time t (min),

$M_\infty$ =the dissolution (%) at infinite time,

$t_0$ =the lag-time (min) of the dissolution,

$\beta$ =shape parameter of the curve,

$\tau_{63.2}$ =time (min) when 63.2% of  $M_\infty$  has been dissolved.

## 4. OBJECTIVES

In the literature overview of the thesis, I summarized the references which are connected with the transdermal delivery and their applications in the pharmaceutical practice. I gave an overview about transdermal delivery devices, especially focused on the matrix type ones. I represented the different polymers which were used to form matrices and enable the drug release from the obtained transdermal systems. The kinetic aspect of the controlled drug release in transdermal therapeutic systems is also presented regarding to their drug depot characteristics.

The objectives of the experimental part of my thesis were:

- to formulate patches containing standard amount of metoprolol tartrate and different amounts of polymers, which are official in the European Pharmacopoeia,
- to characterize *in vitro* the metoprolol tartrate release from the prepared patches,
- to analyze the relationship between the drug release and the composition of the patches regarding to the different polymer ratios,
- to evaluate the applicability and reliability of different kinetic models to describe the drug release from the patches,
- to give a relationship between the drug release and the ability of the polymer matrix to form secondary structures,
- to evaluate in process the patches with appropriate polymer ratio for the desirable drug release by non-invasive FT-IR spectroscopy.

## 5. EXPERIMENTAL PART

### 5.1. *Materials and methods*

#### 5.1.1. Materials

Metoprolol tartrate of Ph. Eur. was selected as a highly water-soluble model drug.

The following excipients were applied for the preformulation examinations and for the preparation of the patches:

- Eudragit RL 30 D (USP/NF, JPE, Ph. Eur.; Evonik Röhm GmbH, Darmstadt, Germany)
- Eudragit RS 30 D (USP/NF, JPE, Ph. Eur.; Evonik Röhm GmbH, Darmstadt, Germany)
- Eudragit NE 30 D (USP/NF, JPE, Ph. Eur.; Evonik Röhm GmbH, Darmstadt, Germany)
- Triethylcitrate (Hungaropharma, Budapest, Hungary)
- Polyethylene glycol (PEG400) (Hungaropharma, Budapest, Hungary)
- Sucrose stearate S1570 (Mitsubishi Chemical Co., Japan)
- Sucrose laurate L1695 (Mitsubishi Chemical Co., Japan)
- Metolose 90 SH 100.000 SR (USP, Ph. Eur.; Shin-Etsu Chemical Company, Tokyo, Japan)
- Metolose SM 4000 (USP, Ph. Eur.; Shin-Etsu Chemical Company, Tokyo, Japan)

#### 5.1.1.1. *Application of metoprolol tartrate*

Metoprolol tartrate is a selective hydrophilic  $\beta$ -blocking agent for the treatment of mild and moderate hypertension and also for long term management of angina pectoris. Metoprolol tartrate is 95% absorbed and has a bioavailability of 40- to 50%. In the blood circulating system it is in the first step 12% protein bound, then rapidly enters the

CNS and has moderate lipid solubility. The metabolism of this drug is hepatically (primarily by CYP2D6). The metabolization occurs also mainly in the liver. Approximately 95% of the drug is excreted renally and less than 5% of the drug is excreted unchanged in urine.

Reduction of exercise induced tachycardia is proportional to the logarithm of the plasma concentration over the range of 20–100  $\mu\text{g/L}$  and effects are detected at 50–100  $\mu\text{g/L}$ . Peak plasma concentrations are achieved after 2–3 hours. Half life of the molecule is 3 to 7 hours. The plasma half-life is about 4 hours [89, 90], which makes frequent dosing necessary to maintain the therapeutic blood levels of the drug for long-term treatment. The n-octanol/water partition coefficient is 0.98 at pH 7.4. Therefore, metoprolol is an ideal drug candidate for transdermal drug delivery. The drug has previously been investigated for its skin permeation potential with menthol as a penetration enhancer [91], as a part of liposomal formulations [8] and also as an active ingredient of transdermal matrix films [92]. Figure 7 shows the structure of metoprolol tartrate.

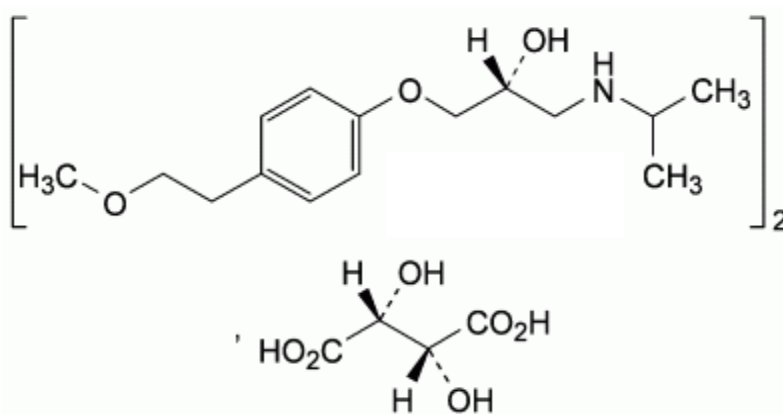
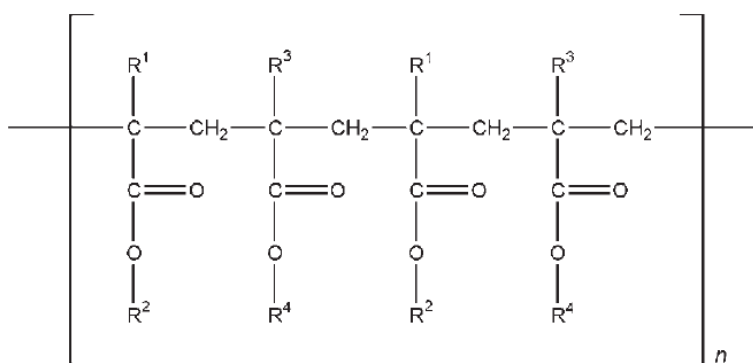


**Figure 7** – Chemical structure of metoprolol tartrate [93]

### 5.1.1.2. Application of acrylates

Acrylic polymers have been known for a long time. They have favorable biocompatibility, good skin adhesion property and good compatibility with a wide range of drugs and excipients.

Polyacrylates are saturated hydrocarbon polymers (Figure 8). Therefore they are highly resistant to oxidation and do not require the addition of stabilizers, the application of which could lead to skin irritation. These polymers are inherently tacky, and therefore, in general they do not need low molecular weight tackifiers and plasticizers to provide the stickiness and softness.



where  $R^1$  is H-,  $CH_3$ -,  $R^2$  is H-,  $CH_3$ -,  $CH_3CH_2$ -,  $CH_2CH_2N(CH_3)_2$ -,  $R^3$  is  $CH_3$ -,  $R^4$  is  $CH_3$ -,  $C_4H_9$ -

**Figure 8** – Chemical structure of acrylic polymers [94]

Poly acrylic esters are produced by copolymerization of acrylic esters, acrylic acid and other functional monomers. Commonly used modifying monomers include vinyl acetate, methyl acrylate, methyl and ethyl methacrylate, acrylic and methacrylic acid, acrylonitrile and certain amine-functional monomers. These modifying monomers can be used to change the solubility and / or permeability of the acrylic polymers. Water-soluble or hydrophilic monomers such as vinylpyrrolidone, 2-hydroxyethyl acrylate and 2-ethyl acrylate have been used to increase the hydrophilicity of the polymers [94].



### 5.1.1.3. *Application of cellulose ether polymers*

Cellulose ethers are derivatives of cellulose. They are formed through partial or total substitution of the hydroxyl groups in the so called etherification. There are different forms of cellulose ethers such as carboxymethylcellulose, methylcellulose, ethylcellulose and hydroxymethyl-, hydroxyethyl- and hydroxypropylcellulose, etc. The physical and chemical properties of cellulose ethers depend on the way and the grade of substitution. Table 1 summarizes the data of the cellulose types which are applied in the preparation of patches.

**Table 1** – Characteristics of the applied Metolose types [95]

<b>Metolose types</b>	<b>Methoxyl content (%)</b>	<b>Hydroxypropoxyl content (%)</b>	<b>Viscosity* (cP)</b>
SM 4000	27.5-31.5	–	3000-5600
90 SH 100.000 SR	19.0-24.0	4.0-12.0	75.000-140.000

\*: USP viscosity

#### 5.1.1.3.1. *Methylcellulose*

Methylcellulose is formed from long-chain substituted cellulose in which approximately 27–32% of the hydroxyl groups are in the form of the methyl ether (Figure 9). The different types of methylcellulose have degrees of polymerization in the range 50–1000, with molecular weights in the range 10.000–220.000 Da. The degree of substitution of methylcellulose is defined as the average number of methoxy (CH<sub>3</sub>O) groups attached to each of the anhydroglucose units along the chain. The degree of substitution also affects the physical properties of methylcellulose, such as its solubility and the viscosity level of solutions, which can be achieved with the application of methylcellulose.

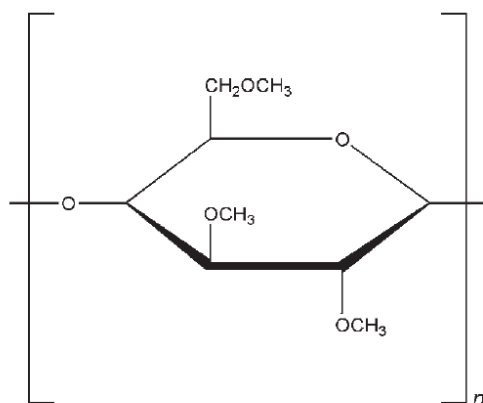


**Figure 9** – Chemical structure of methylcellulose [94]

Methylcellulose is widely used in oral and topical pharmaceutical formulations. The following application forms can occur in tablet formulations:

- binding agents (low- or medium-viscosity grades of methylcellulose). Methylcellulose is added either as a dry powder or in solution [96],
- disintegrants (high viscosity grades of methylcellulose) [97],
- to produce sustained-release preparations,
- to spray-coat (highly substituted low-viscosity grades of methylcellulose) tablet cores to mask unpleasant taste or to modify the release of drug by controlling the physical characteristics of the granules [98],
- to seal tablet cores prior to sugar coating.

In liquid formulations the following application fields are involved:

- emulsify different types of oils (low-viscosity grades of methylcellulose),
- suspend or thicken orally administered liquids (low-viscosity grades of methylcellulose) [99]. Methylcellulose delays the settling of suspensions and increases the contact time of drugs, such as antacids, etc.

In topically applied creams and gels are applied high-viscosity grades of methylcellulose as a thickening agent. In ophthalmic formulations has been also used

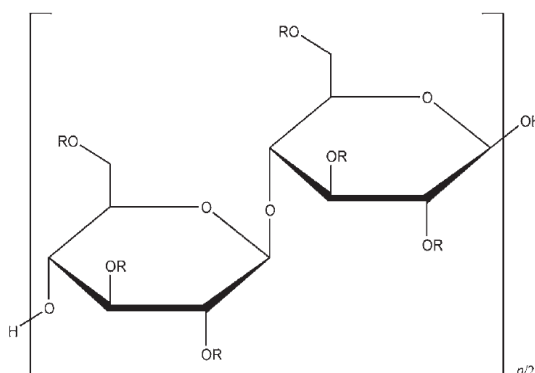
high-viscosity grade of methylcelluloses [100]. Methylcellulose types can be also found in injectable formulations.

Therapeutically, methylcellulose is used as a bulk laxative; it has also been used to aid appetite control in the management of obesity. Practically insoluble in acetone, methanol, chloroform, ethanol (95%), ether, saturated salt solutions, toluene, and hot water. It is soluble in glacial acetic acid and in a mixture of equal volumes of ethanol and chloroform. In cold water, methylcellulose swells and disperses slowly to form a clear to opalescent, viscous, colloidal dispersion.

#### 5.1.1.3.2. *Hypromellose*

Hypromellose is a partly O-methylated and O-(2-hydroxypropylated) cellulose (Figure 10). The different types of hypromellose vary in viscosity and extent of substitution. Grades may be distinguished by appending a number indicative of the apparent viscosity, in mPas, of a 2% w/w aqueous solution at 20°C.

Molecular weight is approximately 10.000–1.500.000.



where R is H-, CH<sub>3</sub>- or CH<sub>3</sub>CH(OH)CH<sub>2</sub>-

**Figure 10** – Chemical structure of hypromellose [94]

These excipients are applied in oral, ophthalmic, nasal, and topical pharmaceutical formulations. In tablet formulations hypromellose is primarily used:

- tablet binder excipient [101],
- film-coating agent [102],

- to form matrix for use in extended release tablet formulations [103, 104],
- to retard the release of drugs from a matrix (at levels of 10-80% w/w),
- to film-coat tablets (at levels of 2-20% w/w).

Hypromellose is also an ideal candidate as a suspending and thickening agent in topical formulations. It is a much better candidate for ophthalmic formulations because of the clarity of solutions made with hypromellose compared with the solutions made with methylcellulose. It forms fewer undissolved fibers. Therefore at low concentration level (0.45–1.0% w/w) hypromellose may be added as a thickening agent for eye drops and artificial tear solutions. It is also used commercially in liquid nasal formulations at a concentration of 0.1% [105]

In topical gels and ointments hypromellose can be applied as an emulsifier, suspending agent, and stabilizing agent. As a protective colloid it can prevent droplets and particles from coalescing or agglomerating. It is also widely used in cosmetics and food products. Hypromellose powder is a stable material, although it is hygroscopic after drying. Solutions are stable at pH 3–11. A reversible sol–gel transformation upon heating and cooling can be observed with hypromellose. The gelation temperature is 50–90°C, depending upon the grade and concentration of this material. Viscosity of the solution decreases as temperature is increased below the gelation temperature, while beyond the gelation temperature viscosity increases as temperature is increased. Aqueous solutions of hypromellose are quite enzyme-resistant, thus provides good viscosity stability during long-term storage [94].

## 5.1.2. Methods

### 5.1.2.1. *Method for preparation of patches*

In the first step, 2/3 part of water was heated to 70 °C. Metoprolol tartrate, the different types of Metolose of various proportions and the different additives were dissolved homogeneously in the hot water. The remaining 1/3 part of the water, stored at 5 °C, was added after homogenizing. This mixture was stirred until dissolving of the components and afterwards it was cooled. At room temperature (25 °C) the different acrylic polymer solutions were added to the system applying a low stirring rate to avoid forming of air bubbles.

This preparation method enabled that metoprolol tartrate is completely dissolved before embedded in the matrix and is fully dispersed in the polymer system in the course of the drying process. In the cooling step of the preparation of the patches, there is an increase in the viscosity of the solution containing Metolose, which makes more difficult to mix it with the polyacrylate solution thoroughly.

The homogenous mixture was filled into a gum ring of a constant diameter (54 mm). Each sample contained 7.5 g of this mixture. The metoprolol tartrate concentration of the mixture was 1.11% w/w in each sample. The drying of the samples was performed at room temperature for a 3 day period. The further investigations were done after this 3 day period. First the thickness of patches was checked and in each formulation was found similar.

### 5.1.2.2. *Organoleptic examination of different compositions for preparing applicable patches*

For the determination of the incompatibility between the model drug and the polymer matrix forming components I prepared patches and after 3 days of storage in exsiccator with organoleptic observation I chose the macroscopically homogeneous candidates for further examinations.

### 5.1.2.3. *Viscosity measurements*

The prepared gel formulations at room temperature were filled into the cylinder of the viscosimeter (HAAKE VT550 Rheometer, Haake GmbH, Karlsruhe, Germany). The

measurements were done at 25°C. For the evaluation the balance viscosity values of each formulation (n=3) were taken. The viscosity – time curves were recorded with the following parameters: disc SV2, G= 50 1/min, measurement time was 15 min.

5.1.2.4. *Optimization of composition according to the drug liberation examinations*

This test was performed by Hanson SR8-Plus (Hanson Research, Chatsorth, USA) according to Ph. Eur. regulation – Paddle over disk. TTS samples after 3 days of storage were placed into a disk apparatus. Then they were immersed into the temperature-controlled 400 ml acceptor medium (pH = 6.00 buffer solution). The acceptor medium was kept at  $32 \pm 1^\circ\text{C}$  and mixed at the rate of 25 rpm with rotating pad. Samples were taken at predetermined time points with AutoPlus Maximizer system and an Auto Plus MultiFill collector (Hanson Research, Chatsorth, USA). The sample volume was 10 ml, which was replaced each time with the equivalent of dissolution medium. The active content of the samples was determined with an Auto Plus On-Line UV/VIS Autosamples spectrophotometer at 274 nm on the basis of a calibration curve recorded earlier. The examination cell is shown in Figure 11.

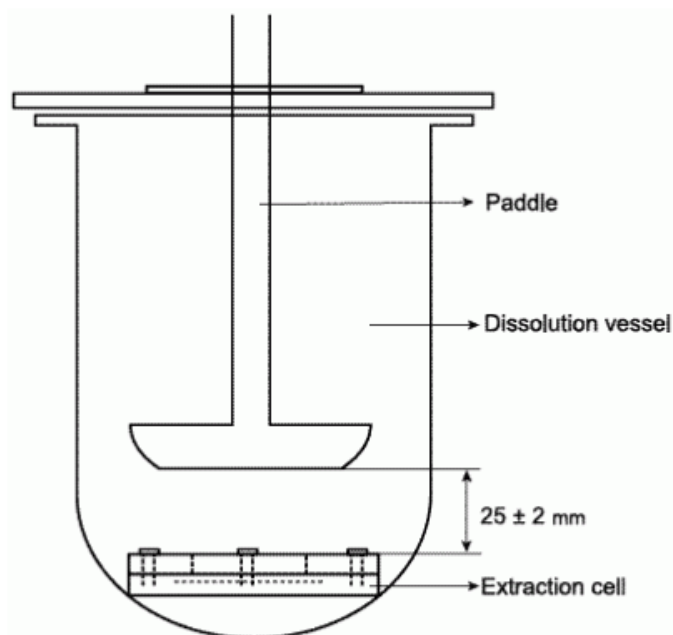


**Figure 11** – Drug liberation examination cell [93]

#### 5.1.2.5. *Analysis of the release profiles according to different kinetic models*

The following mathematical models were evaluated considering the drug release profiles of the patches. The non-linear parameter estimation of the release models applied for matrices was made with the Solver function of the computer package Microsoft Excel 5.0.

In the evaluation of the matrices we applied the following models:

zero-order model

first-order model

Weibull distribution.

#### 5.1.2.6. *FT-IR examinations*

FT-IR spectra of the cast film patches were obtained using a JASCO FT/IR-4200 spectrometer in 4000-400  $\text{cm}^{-1}$  wavenumber range. 32 scans were performed at a resolution of 4  $\text{cm}^{-1}$ . The system was operated in the transmission mode. Spectra Analysis software was applied for the determination of the peak area within the wavenumber range of 1757.7-2811.8  $\text{cm}^{-1}$ .

#### 5.1.2.7. *Non-invasive stability screening of patches with ATR-FTIR examinations*

The prepared matrices with and without metoprolol tartrate were stored 1 month at  $40\pm 2^\circ\text{C}$  and  $75\pm 5\%$  relative humidity in open container.

The ATR-FTIR spectra of the stored patches with and without metoprolol tartrate samples were scanned over wavenumber range of 4000–600  $\text{cm}^{-1}$  using Able Jasco FT-IR 4200 type A spectrometer with ATR Pro470H single reflection ATR accessory. 32 scans were performed at a resolution of 4  $\text{cm}^{-1}$ .

#### 5.1.2.8. *Positron annihilation lifetime spectroscopy (PALS)*

Positron annihilation lifetime spectroscopy (PALS) is a unique method since it is exceptionally sensitive to the free volume. It is frequently used to determine the size distribution of free volume holes in polymers. All of these measurements are based on

the interaction of the free volume holes and the so called *ortho*-positronium atom.

When positrons are injected to an amorphous molecular material they form three different states in the simplest case. A part of them forms positronium (Ps) atoms with the electrons of the material. This exotic atom, which is the bound state of an electron and a positron, has two ground states depending on the relative orientation of the spins of the constructing particles. The *para*-Ps, in which the spins are anti-parallel, has a very short intrinsic lifetime (125 ps). The usual reactivity of Ps atoms is not very high and in most of the cases the two particles bound in *para*-Ps (the positron and the electron) annihilate with each other by the intrinsic lifetime ( $\tau_1$ ). The other ground state of positronium is the *ortho*-Ps (o-Ps), in which the spins are parallel. This Ps state has a very long lifetime in a vacuum (141 ns) and, even at very low reactivity, it interacts with the electrons of the surrounding material considerably. Usually the positron of the *ortho*-Ps does not annihilate with its own electron but rather with an electron of the material. This interaction decreases the intrinsic lifetime significantly and usually a much shorter lifetime is observed (1-10 ns). Even so, this is the longest lifetime component of positron lifetime spectra ( $\tau_3$ ).

The third state of positrons in materials is usually due to positrons not able to form Ps atoms. These positrons diffuse almost freely in the material but they should also annihilate sooner or later with surrounding electrons, i.e., with the electrons of polymeric chains in our case. This provides a medium long lifetime ( $\tau_2$ ) that characterizes the average electron density of the material. This lifetime component usually reflects tiny changes of the electron structure of a material very sensitively. In amorphous materials as polymers the size of free volume holes is not uniformly distributed. Consequently, the simple assumption on the number and the nature of positron states is not necessarily correct. In these materials, instead of one well defined o-Ps state, a number of similar states occur depending on the size of the free volume around the positronium. So the lifetime spectrum,  $S(t)$  is not a simple sum of exponential curves and instead of:

$$S(t) = \sum_i A_i \exp(-\lambda_i t) \quad (8)$$

it can be described by a continuous distribution of lifetimes:



$$S(t) = \int_0^{\infty} h(\lambda) \exp(-\lambda t) d\lambda \quad (9)$$

where  $\lambda_i$ -s are the assumed separate lifetimes,  $A_i$ -s are their relative intensities, while the function  $h(\lambda)$  is the lifetime distribution function which is proportional with the size distribution of free volume holes in the material.

In polymers the formed o-Ps atoms tend to be trapped in free volume holes and, as mentioned above, their annihilation is not governed by their intrinsic lifetime but by the electron density in the holes. Their lifetime is associated with the size of the free volume around them:

$$\tau = \frac{R^2}{2D} \left( 1 - \frac{R}{\Delta R} \right) \quad (10)$$

where  $\tau$  is the positronium lifetime,  $R$  is the radius of the free volume hole, and  $\Delta R$  is a constant. Consequently, on the basis of o-Ps lifetime distributions we gain a detailed picture on the size distribution of free volume holes [106, 107].

The positron source applied for the measurements was made of carrier free  $^{22}\text{NaCl}$  of the activity of  $4 \times 10^5$  Bq. The active sodium chloride was sealed between two very thin kapton foils. The source was then placed between two pieces of the sample treated identically before. Positron lifetime spectra were recorded by a conventional fast-fast coincidence system. The system was constructed from standard ORTEC electronic units, while the detectors from  $\text{BaF}_2$  scintillator crystals and XP2020Q photomultipliers. The time resolution of the system was about 200 picoseconds. The spectra were evaluated into three lifetime components. The two shorter lifetime components (165ps, 460ps) are mixtures of different positron and positronium states. As they are too complicated to interpret physically, they were ignored in the evaluations. The longest living positron state is due to ortho-positronium. The lifetime of this positronium state is, in the case of polymers, connected with the size of free volume holes [108]. The longer this lifetime, the larger the holes are.

## 5.2. RESULTS

### 5.2.1. Preformulation examinations

#### 5.2.1.1. *Preparation of Eudragit films for further formulation of matrices containing metoprolol tartrate*

The aim of the preformulation examinations was to create matrix type patches with the combination of polyacrylate polymer and different additives to embed the model drug (metoprolol tartrate). For this reason there were investigated several types of polyacrylate polymer solutions in combination with metoprolol tartrate for compatibility. For these examinations I prepared different samples with Eudragit RL 30 D, Eudragit RS 30 D and Eudragit NE 30 D with different additive such as triethyl-citrate, PEG400, Sucrose stearate S1570, Sucrose laurate L1695. Acrylates are suitable to formulate oral dosage forms which are able to release their content in different parts of the GI tract. According to their functional groups they can influence at which pH values they swell and get permeable. There are also several types which enable the applied drugs to be released with time control under independent pH values [109]. There can be found several examples in the literature for the application of Eudragit polymers to formulate transdermal matrices: mainly the following two types are mentioned as a part of matrix formulations: Eudragit RS and Eudragit RL [110-114]. These two types have trimethyl-ammonioethylmethacrylate as functional group which enables high permeability and pH independent swelling. The application of Eudragit NE 30 D (aqueous dispersion of a neutral copolymer based on ethyl acrylate and methyl methacrylate) in matrix type patches can be also advantageous, because of its time-controlled drug release properties [69, 115, 116]. For the formulation of matrices these 3 types were chosen.

The aim of the first formulations in the developing of matrices was to obtain structures which can be manufactured with film casting method resulting in patches which are flexible and applicable on the skin. Eudragit RS and Eudragit RL were applied for preparing matrices alone and also with different plasticizers. The summary of formulations can be seen in Table 2.

**Table 2** – Patches with different acrylate components and different additives on wet

Sample number / Components	basis (% w/w)							Remark
	Eudragit RS 30 D	Eudragit RL 30 D	Eudragit NE 30 D	Triethyl-citrate	PEG 400	Sucrose stearate S1570	Sucrose laurate L1695	
Polymer content (% w/w)								
1.	30.00	-	-	-	-	-	-	rigid
2.	28.57	-	-	-	4.76	-	-	rigid
3.	27.27	-	-	-	9.09	-	-	rigid
4.	26.09	-	-	-	13.04	-	-	rigid
5.	25.00	-	-	-	16.67	-	-	rigid
6.	24.00	-	-	-	20.00	-	-	rigid
7.	23.08	-	-	-	23.08	-	-	rigid
8.	22.22	-	-	-	25.93	-	-	rigid
9.	21.43	-	-	-	28.57	-	-	rigid
10.	-	30.00	-	-	-	-	-	rigid
11.	-	28.57	-	-	4.76	-	-	rigid
12.	-	27.27	-	-	9.09	-	-	rigid
13.	-	26.09	-	-	13.04	-	-	rigid
14.	-	25.00	-	-	16.67	-	-	rigid
15.	-	24.00	-	-	20.00	-	-	rigid
16.	-	23.08	-	-	23.08	-	-	rigid
17.	-	22.22	-	-	25.93	-	-	rigid
18.	-	21.43	-	-	28.57	-	-	rigid
19.	28.57	-	-	1.43	-	-	-	rigid
20.	27.27	-	-	2.73	-	-	-	flexible
21.	26.09	-	-	3.91	-	-	-	flexible
22.	25.00	-	-	5.00	-	-	-	flexible
23.	24.00	-	-	6.00	-	-	-	flexible
24.	23.08	-	-	6.92	-	-	-	flexible
25.	22.22	-	-	7.78	-	-	-	flexible
26.	21.43	-	-	8.58	-	-	-	flexible
27.	-	28.57	-	1.43	-	-	-	rigid
28.	-	27.27	-	2.73	-	-	-	flexible
29.	-	26.09	-	3.91	-	-	-	flexible
30.	-	25.00	-	5.00	-	-	-	flexible
31.	-	24.00	-	6.00	-	-	-	flexible
32.	-	23.08	-	6.92	-	-	-	flexible
33.	-	22.22	-	7.78	-	-	-	flexible
34.	-	21.43	-	8.58	-	-	-	flexible
35.	-	29.93	-	-	-	0.25	-	rigid
36.	-	29.85	-	-	-	0.50	-	rigid
37.	29.93	-	-	-	-	0.25	-	rigid
38.	29.85	-	-	-	-	0.50	-	rigid
39.	-	29.93	-	-	-	-	0.25	rigid
40.	-	29.85	-	-	-	-	0.50	rigid
41.	29.93	-	-	-	-	-	0.25	rigid
42.	29.85	-	-	-	-	-	0.50	rigid
43.	-	-	30.00	-	-	-	-	flexible

### 5.2.1.2. Optimization of formulations using different Metolose types

Different matrix type patches were created for the further examinations with Eudragit NE 30 D and with different types of Metolose (Table 3) and with different additives. Figure 12 illustrates the release profiles of the different samples on wet basis.

**Table 3** – Preformulation examinations of different excipients for preparing patches on wet basis (% w/w)

Components / Sample number	44	45	46	47	48
Metoprolol tartrate	1.11	1.11	1.11	1.11	1.11
Eudragit NE 30 D (polymer content)	6.67	6.67	6.67	6.67	6.67
Metolose SM 4000	2.00	2.00	2.00	1.60	1.00
Metolose 90 SH 100.000 SR	0.00	0.00	0.00	0.40	1.00
Sucrose stearate S1570	0.00	0.80	0.00	0.00	0.00
Sucrose laurate L1695	0.00	0.00	2.00	0.00	0.00

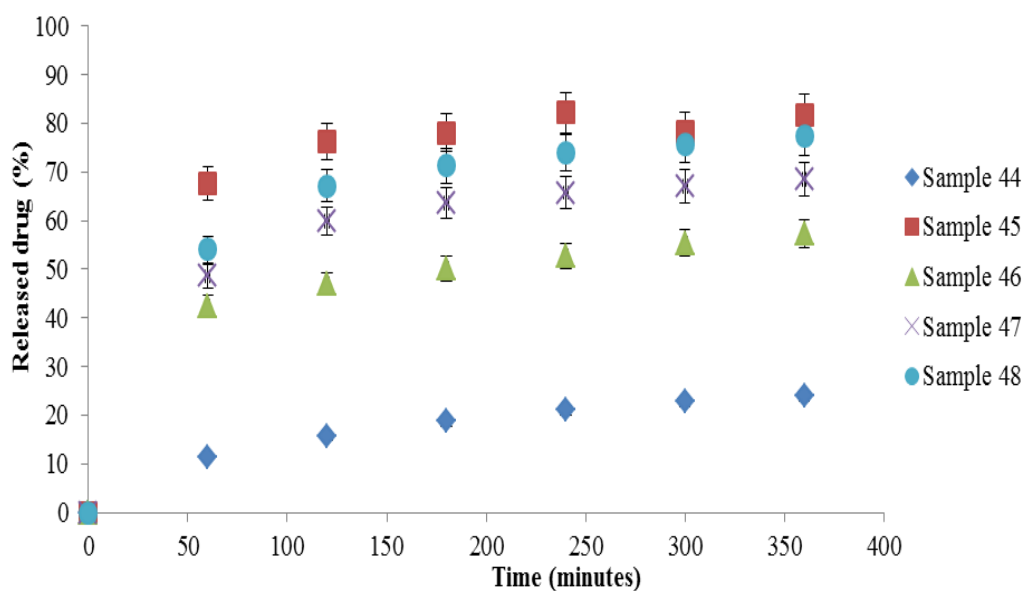


**Figure 12** – Drug release of patches with different additives (n=3, RSD<5%)

### 5.2.1.3. *Viscosity aspects for the preformulations*

During the preparation of the patches in the cooling process, there can be observed a big increase in the viscosity of the solution containing the different Metolose types and the active ingredient. This increase makes more difficult to make a homogenous, totally dispersed system in which the active ingredient is also totally dispersed. Figure 13 and 14 represent the viscosity effect on the solution of the two Metolose types in different concentrations, respectively the additional effect of the metoprolol tartrate was also investigated.

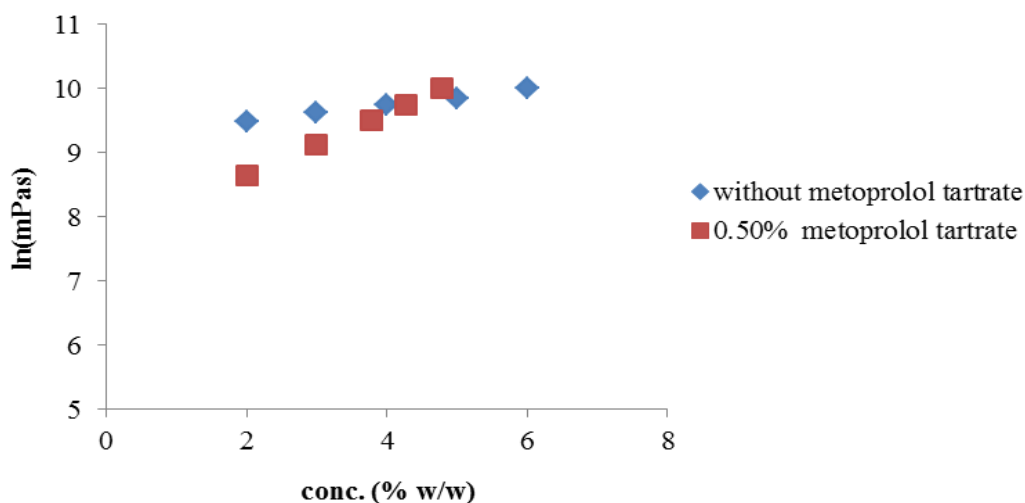


**Figure 13** – Viscosity profile of the solution containing Metolose SM 4000 (n=3, RSD<5%)

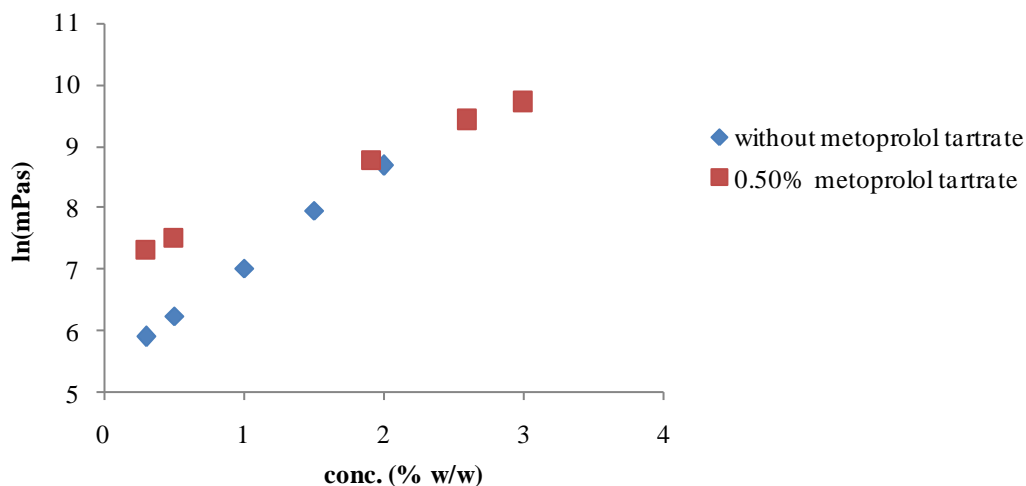


**Figure 14** – Viscosity profile of the solution containing Metolose 90 SH 100.000 SR  
(n=3, RSD<5%)

## 5.2.2. Results of the analysis of the TTS systems

### 5.2.2.1. Drug liberation examinations

To analyze the effect of the Metolose components of the matrix type patches on drug liberation there were investigated the following formulations included in Table 4. The composition of each patch is represented on wet and on dry basis (w/d, % w/w). Table 5 summarizes the kinetic data of the different formulations evaluated by using the Weibull method. On the base of the release profile, zero-order model and first-order model cannot be applied for the evaluation of the kinetic properties of each patch. The calculations assume that the whole drug amount will be totally released from the patches into the acceptor medium. Figure 15 illustrates the drug release profile of the different formulations in the acceptor medium (pH=6.00).

**Table 4** – Patches with different Metolose contents on wet and on dry basis (% w/w)

Components / Sample number	49	50	51	52	53	54
Metoprolol tartrate	1.11/11.08	1.11/11.02	1.11/11.05	1.11/10.82	1.11/10.81	1.11/10.90
Eudragit NE 30 D (polymer content)	6.67/66.57	6.67/66.21	6.67/66.37	6.67/65.02	6.67/64.96	6.67/65.50
Metolose SM 4000	2.00/19.96	1.80/17.87	1.60/15.92	1.40/13.65	1.20/11.69	1.00/9.82
Metolose 90 SH 100.000 SR	0.00/0.00	0.20/1.99	0.40/3.98	0.60/5.85	0.80/7.79	1.00/9.82
Water	90.22/2.40	90.22/2.92	90.22/2.68	90.22/4.66	90.22/4.75	90.22/3.96

**Table 5** – Kinetic parameter of patches according to the Weibull method

Sample number	$\tau_{63.2}$ (min)	$t_0$	$\beta$	$R^2$
49	4087.58	0.00	0.51	0.995
50	905.23	0.00	0.58	0.994
51	189.53	0.00	0.42	0.966
52	178.61	0.00	0.46	0.973
53	150.17	0.00	0.59	0.993
54	121.54	0.00	0.55	0.968

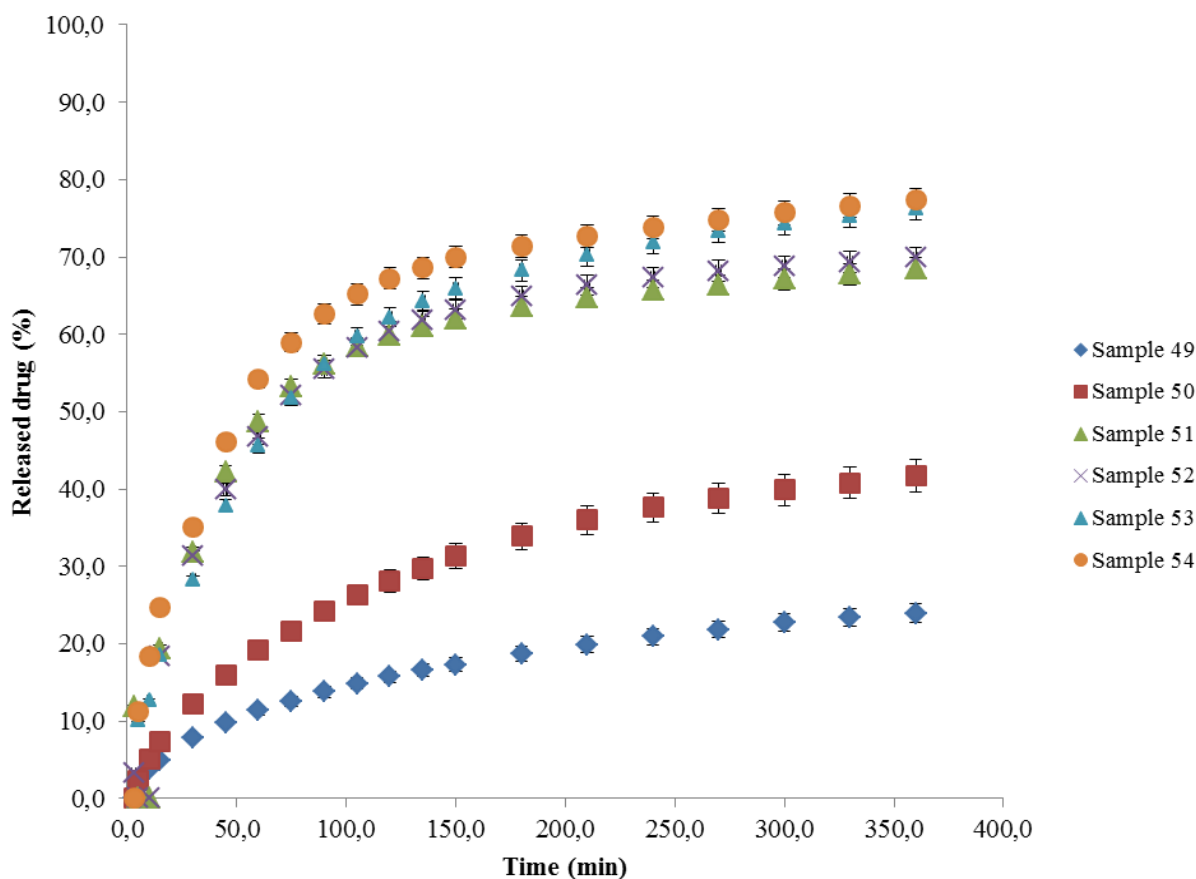


**Figure 15** – Drug release profile of patches containing different proportions of polymers (n=3, RSD<5%)

#### 5.2.2.2. Storage of patches

Metoprolol tartrate can be stored as a free drug for a long period of time without any chemical and physical degradation. Similar results have been found in matrix type matrices. These matrices contained metoprolol tartrate, polyacrylic polymer, polyvinyl alcohol [117, 118].

Each formulation was stored under stress conditions at  $40\pm 2^{\circ}\text{C}$  and  $75\pm 5\%$  relative humidity in open container. ATR-FTIR spectroscopy was applied to detect the stability changes of intact patches in the course of storage. Figure 16 illustrates the ATR-FTIR spectra of one combination of patches (Sample 53). After 1 month of storage, neither in the spectra of patches containing metoprolol tartrate nor in those without the active agent any other peak could be identified. Figure 17 represents the spectra of Sample 52 without storage and with one month of storage.



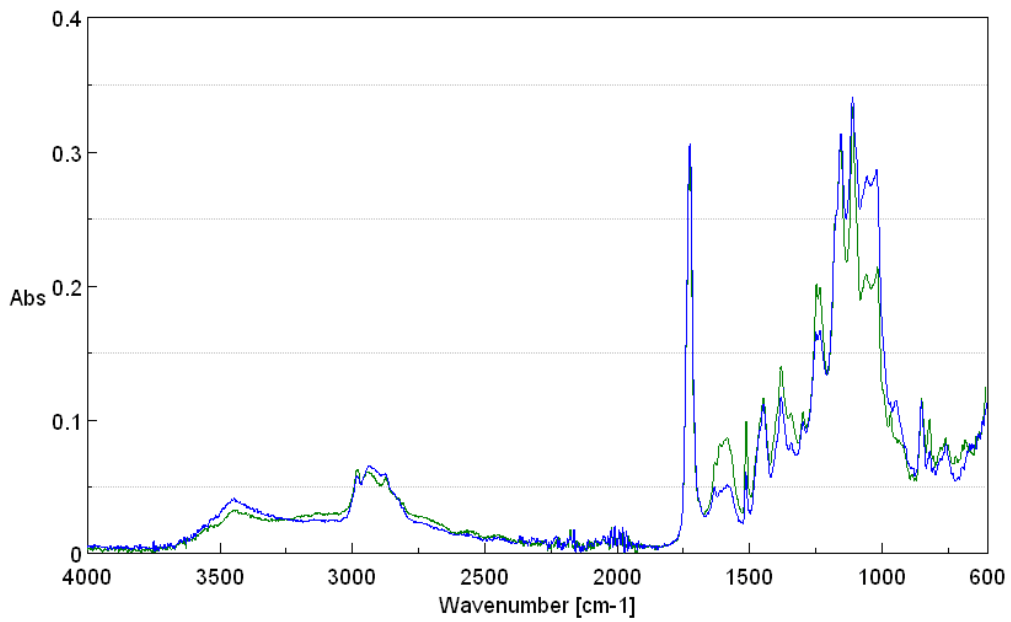


**Figure 16** – Comparison of the ATR-FTIR spectra of the patches (Sample 53) containing metoprolol tartrate (green spectra) and without metoprolol tartrate (blue spectra)

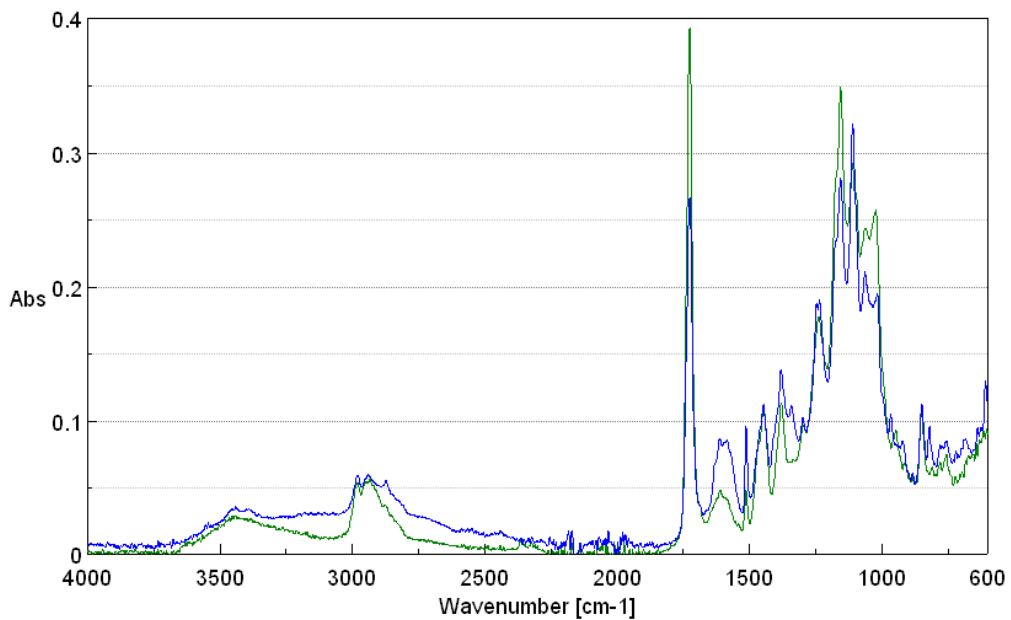


**Figure 17** – Comparison of the ATR-FTIR spectra of the patches (Sample 52) containing metoprolol tartrate with storage (blue spectra) and without storage (green spectra)

### 5.2.2.3. *FT-IR examinations*

I investigated how the drug release and FT-IR characteristics of Metolose patches were influenced by the changes of Metolose SM 4000 (methylcellulose) and Metolose 90 SH 100.000 SR (hypromellose) proportions. FT-IR spectroscopy measurements were performed in parallel with the metoprolol tartrate release study to track the effect of the composition on the drug release.

The characteristic FT-IR peaks of metoprolol tartrate are summarized in Table 6. The presence of metoprolol tartrate could be identified according to its characteristic peaks in those spectra of patches containing the drug (Figure 18).

**Table 6** – Vibrational band assignment for metoprolol tartrate [119]

Frequency (cm <sup>-1</sup> ) FTIR	Vibrational band assignment
3459 (w)	N-H stretching
3033 (w)	O-H stretching
2983 (m)	N-H/C-H symmetric stretching
2938 (w)	C-H stretching
2875 (m)	C-H stretching
2813 (w)	C-H stretching of CH <sub>2</sub> group
2745 (vw)	N-H symmetric stretching
2572 (vw)	N-H stretching
2552 (w)	N-H stretching
2452 (w)	O-H stretching
1590 (s)	CO <sub>2</sub> antisymmetric stretching
1514 (s)	CO <sub>2</sub> asymmetric stretching
1460 (m)	O-H/C-H deformation
1400 (m)	Aromatic ring stretching
1358 (m)	CH <sub>3</sub> deformation
1300 (m)	O-H deformation
1250 (s)	O-H deformation
1235 (m)	C-N deformation
1181 (m)	C-O stretching
1164 (m)	C-O antisymmetric stretching
1112 (s)	C-O asymmetric stretching
1074 (w)	Aromatic ring stretching
1054 (m)	C-O stretching
1014 (m)	C-O deformation
967 (m)	O-H deformation
935 (m)	out of plane O-H vibration of carbonyl group
821 (s)	out of plane O-H vibration of carbonyl group
780 (w)	Liberation of H <sub>2</sub> O
686 (m)	out of plane O-H vibration of alcohol
605 (m)	out of plane O-H vibration of alcohol
542 (m)	O-H torsional vibration
508 (m)	CO <sub>2</sub> deformation

s-strong, m-medium, w-weak, vs-very strong, vw-very weak

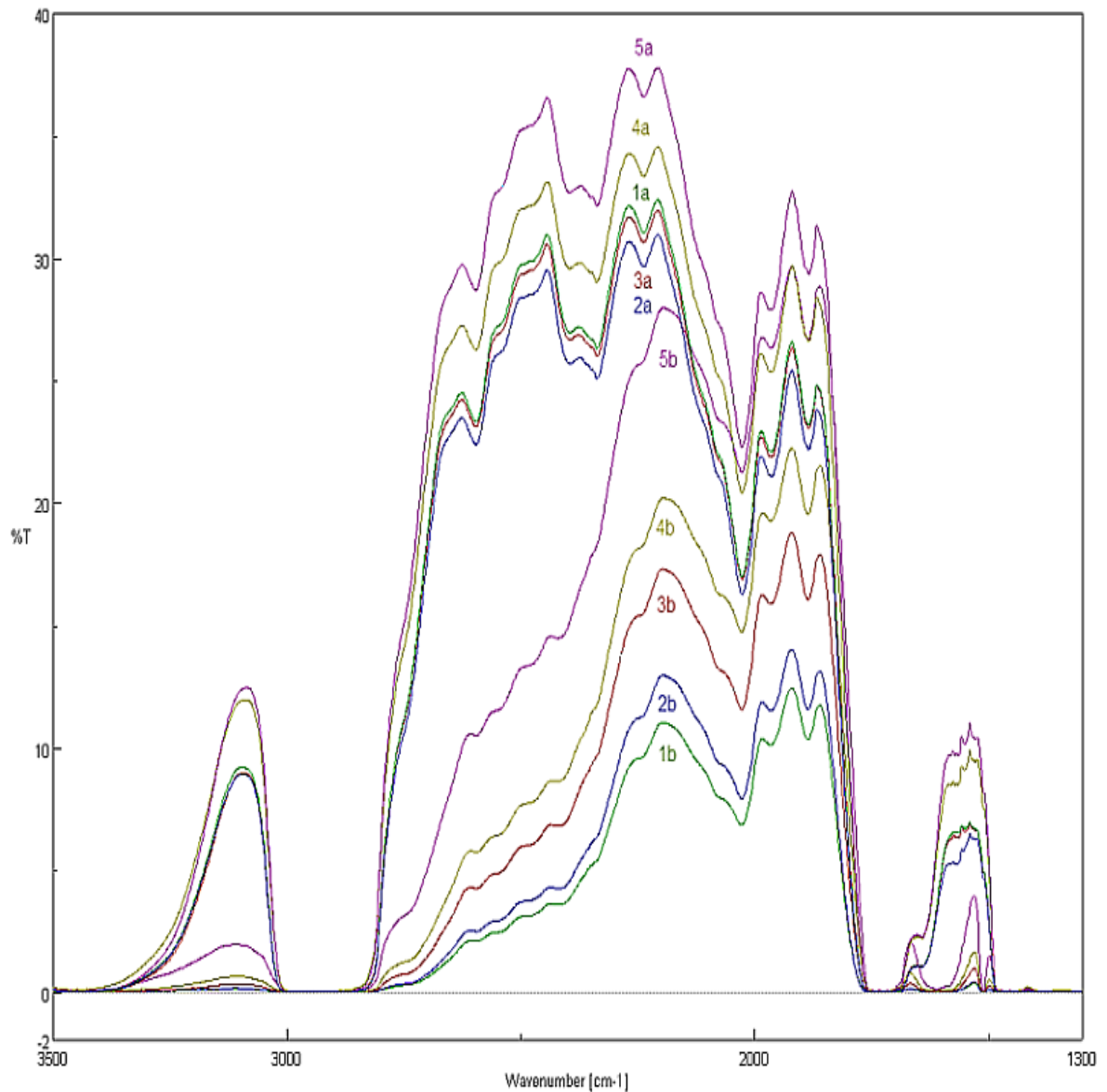


**Figure 18** - FT-IR spectra of different patches with metoprolol tartrate

Sample 50 - Metolose SM 4000 concentration 1.80% (AUC=5919.2)-1 a, b

Sample 51 - Metolose SM 4000 concentration 1.60% (AUC=6783.9)-2 a, b

Sample 52 - Metolose SM 4000 concentration 1.40% (AUC=10034.2)-3 a, b

Sample 53 - Metolose SM 4000 concentration 1.20% (AUC=12333.7)-4 a, b

Sample 54 - Metolose SM 4000 concentration 1.00% (AUC=18167.2)-5 a, b

Spectra with “a” are the spectra of blank patches, while spectra with “b” are the spectra of patches with metoprolol tartrate

5.2.2.4. *Positron annihilation lifetime spectroscopy (PALS)*

Figure 19 represents the o-Ps lifetime distribution in 3 samples. Compositions see in Table 4.

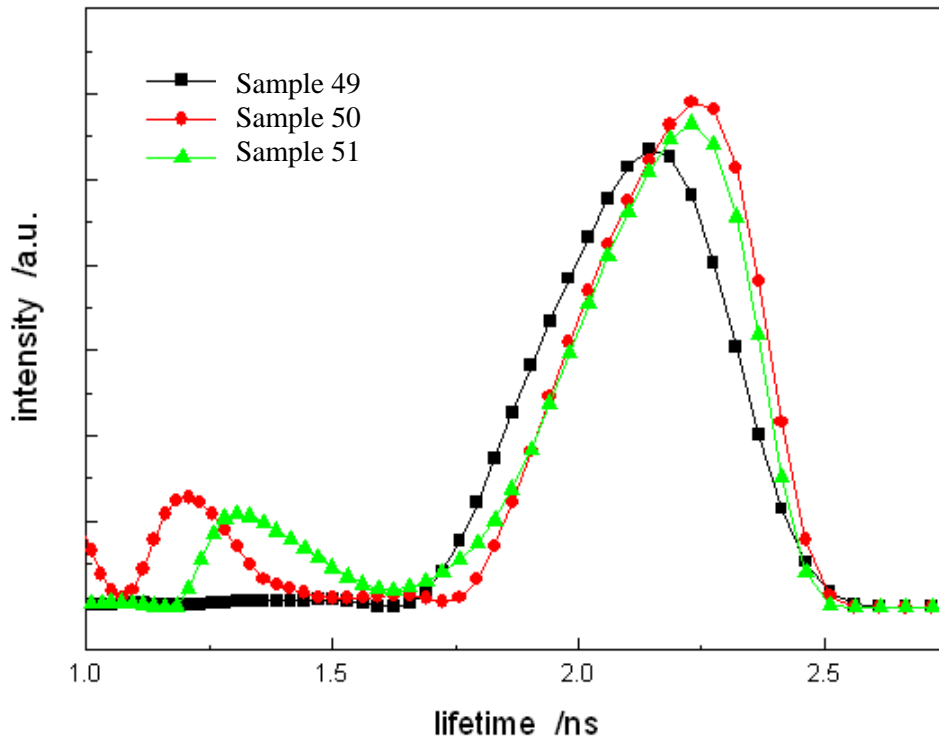


**Figure 19** – o-Ps lifetime distribution in different samples (n=3)

### 5.3. *DISCUSSIONS*

#### 5.3.1. Formulation considerations of applicable patches

According to the results of the preformulation examinations (Table 2) the application of triethylcitrate with Eudragit RS 30 D and Eudragit RL 30 D in appropriate amount resulted in flexible matrices. These formulations were then prepared with metoprolol tartrate (applied amount of drug was: 1.11 w/w % on wet basis) to investigate the drug release profile of patches (Sample 20 and 28). Drug release measurements showed that the drug could not liberate from these two compositions.

For further examinations we have chosen Eudragit NE 30 D because this polyacrylate polymer does not require any additional plasticizer or the application of lower amount of plasticizer can ensure similar physicochemical characteristics like in the case of Eudragit RS 30 D and RL 30 D. Sample 43 was then prepared with metoprolol tartrate (applied amount of drug was: 1.11 w/w % on wet basis) to examine the drug release profile of patches. The measurements showed that no drug could liberate from this composition.

Eudragit NE was afterwards combined in different proportions with Metolose SM 4000. During the optimization of formulations (Table 3) using different Metolose types the different compositions show different release profiles (Figure 12). It can be observed that the combination of Eudragit NE 30 D and Metolose SM 4000 leads to very low drug release, so this formulation needs to be modified with other components. In the case of application of Sucrose stearate S1570, there is a great increase of released drug, however, in the 1. hour already 67.7% of the drug amount is released. The application of Sucrose laurate L1695 leads to the increase of the released drug, but only 57.7% of the whole drug amount is released in the 6. hour of examination. The application of plasticizers resulted in a great increase of released drug without any possibility for the modification in the kinetics of the drug release. In the case of Metolose 90 SH 100.000 SR it can be observed that the released drug amount can be modified with the different amounts of Metolose 90 SH 100.000 SR. According to the results of the drug liberation, we found that the application of Eudragit NE 30 D, Metolose SM 4000 and Metolose 90

SH 100.000 SR can be used for preparing matrix type patches containing metoprolol tartrate.

Viscosity data (Figure 13 and Figure 14) showed, that the application of metoprolol tartrate in smaller concentrations has effect on the viscosity in the case of both cellulose polymers. It leads at low concentration level of Metolose 90 SH 100.000 SR to small increase of viscosity and at low concentration level of Metolose SM 4000 it tends to lower the viscosity of the solution. The application level of Metolose 90 SH 100.000 SR increases much more intensively the viscosity of the solution, which results in a lower application level of this polymer for preparing the patches. On the grounds of the viscosity measurements and the empirical experiences, Metolose 90 SH 100.000 SR can be applied up to 1.0% w/w, Metolose SM 4000 can be used up to 2.0% w/w for the preparation of the patches.

### 5.3.2. Kinetic considerations of the release profiles

As discussed above, the applied polymers alone were not able to form adhesive and flexible patches of controlled drug release, thus a mixture of Eudragit NE 30 D and two types of Metoloses were used to obtain the required characteristics. Compositions see in Table 4. The water insoluble, pH independent, water swellable, and water permeable Eudragit NE 30 D enables the barrier function of the homogeneous polymer composite. Since the concentration of the Eudragit NE 30 D was kept constant in each patch (6.67% w/w on wet basis), the drug release profile was controlled by the various proportions of water-soluble Metolose SM 4000 and Metolose 90 SH 100.000 SR. No lag-time ( $t_0 = 0$ ) values were detected (Figure 15).

The extending ratio of Metolose 90 SH 100.000 SR enables higher extent of metoprolol tartrate release, which indicates that the presence of the hydroxypropoxyl groups in the polymer matrix facilitates and controls the drug release. Table 5 shows, that the increased ratio of the hydroxypropoxyl groups had no significant effect on the value of the shape parameter ( $\beta$ ). Since the  $\beta$  values were within 0.42 and 0.59 in the case of each patch, the metoprolol tartrate release followed Fickian diffusion. Hydroxyl groups are able to form H-bonds with the water while methoxyl groups are not. This explains the change of drug release profile of the studied polymers. The higher the proportion of

Metolose SM 4000 in the patches, the less the interaction between the water and the polymer is. The formation of H-bonds, consequently the water penetration through the polymeric patch is more supported with the application of Metolose 90 SH 100.000 SR thus increasing the extent and rate of metoprolol tartrate release from the patches. The initial slower release refers to the formation of H-bonds due to the swelling process.

### 5.3.3. Non-invasive stability screening of patches

Figure 16 illustrates the ATR-FTIR spectra of one combination of patches (Sample 53). These spectra were made after 1 month of storage. The presence of metoprolol tartrate can be identified primarily with the characteristic peak at  $1507\text{ cm}^{-1}$  which could refer to the  $\text{CO}_2$  asymmetric stretching in the molecule. This peak can be identified in all samples containing the drug; other peaks interfere with the functional groups of the polymer matrix and cannot clearly characterize the functional groups of metoprolol tartrate. The most characteristic peak of the patch can be found at  $1726\text{ cm}^{-1}$ . This peak can be also identified in each formulation. After 1 month of storage, neither in the spectra of patches containing metoprolol tartrate nor in those without the active agent any other peak could be identified. Figure 17 represents the spectra of Sample 52 without storage and with one month of storage. There can be observed any other peak in both spectra. The results enable quick non-destructive stability screening of patches. According to these results the samples can be found stable during the period of observation, which is in good compliance with the results found in the literature background.

### 5.3.4. Relationship between FT-IR spectra and kinetic data of patches

The characteristic FT-IR peaks of metoprolol tartrate are summarized in Table 6. The presence of metoprolol tartrate could be identified according to its characteristic peaks in those spectra of patches containing the drug.

Figure 18 illustrates the FT-IR spectra of blank patches and of that containing metoprolol tartrate. The different compositions see in Table 4. Characteristic peaks at  $1867\text{ cm}^{-1}$ ,  $1922\text{ cm}^{-1}$ , and  $1987\text{ cm}^{-1}$  wavenumbers were found independently from the



presence of metoprolol tartrate, which refer to the carbonyl group of methacrylate ester copolymer. Characteristic peaks could be observed at  $2208\text{ cm}^{-1}$ ,  $2270\text{ cm}^{-1}$ ,  $2444\text{ cm}^{-1}$  and  $2626\text{ cm}^{-1}$  wavenumbers in each blank patch, which could be attributed to the ester groups derived from Metolose SM 4000 and Metolose 90 SH 100.000 SR. These peaks were disappeared in the presence of metoprolol tartrate. Only one new peak appeared at  $2196\text{ cm}^{-1}$  referring to the aromatic ring of metoprolol tartrate.

A broad hydroxyl absorption band was found at  $3087\text{ cm}^{-1}$  indicating the presence of hypromellose. The signs of the OH bands will be much more intensive with the growing ratio of hypromellose. The latter was dominant in the empty patches. In the presence of metoprolol tartrate the specific absorption band disappeared. The possible explanation for this phenomenon could be the interaction between the polymer and metoprolol tartrate forming homogenous polymeric composite patches in which metoprolol tartrate is entrapped.

The increase of the transmission values of the characteristic peaks along with the Metolose 90 SH 100.000 SR content indicates the microstructural changes of the patches via H-bridges with the OH groups of Metolose 90 SH 100.000 SR. Since no extraneous peaks were found, the spectra are masking-like and feasible to make quantitative analysis due to their positions in the analytical wavenumber range. This non-invasive quantitative analysis of patches is based on the determination of the AUC values measured within the characteristic wavenumber range.

Linear relationship was found with good correlation ( $R= 0.9380$ ) between the area under the peak values of the FT-IR curves of Metolose containing patches measured within the wavenumber range of  $1757.7\text{-}2811.8\text{ cm}^{-1}$  and the  $\log \tau_{63.2}$  values ( $y$ ) of metoprolol tartrate release [120].

Figure 20 illustrates the correlation between the peak area and the  $\log \tau_{63.2}$  values of Metolose patches containing metoprolol tartrate.

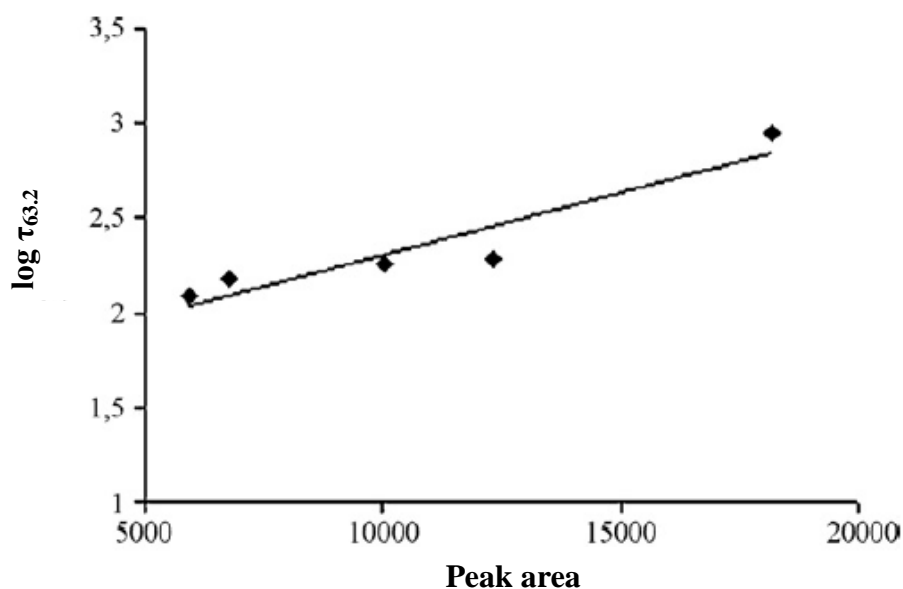


**Figure 20** - Correlation between the peak area measured within the wavenumber range and the  $\log \tau_{63.2}$  values of Metolose patches containing metoprolol tartrate

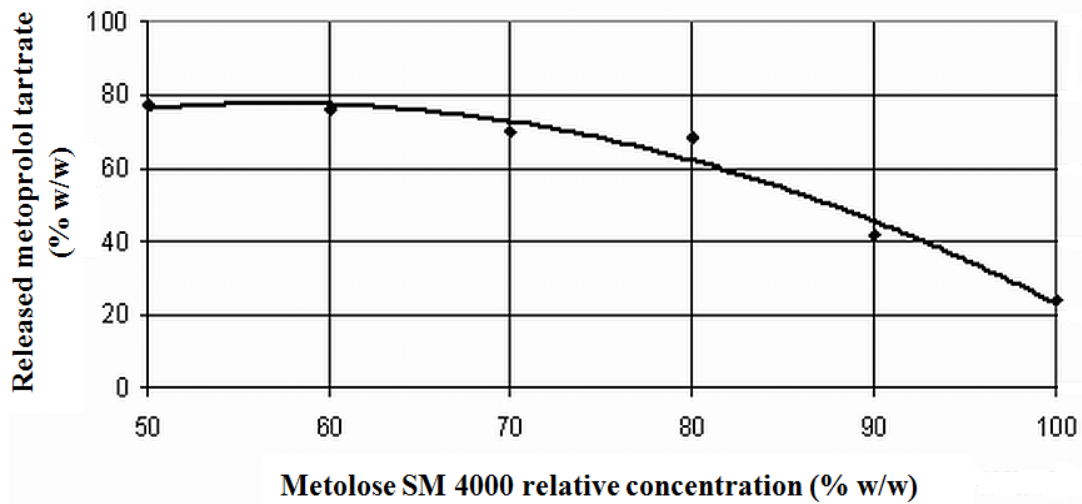
On the basis of our results, the application of FT-IR measurements can be recommended as a useful non-destructive means during the in-process control of patches.

### 5.3.5. Aspects of the positron annihilation lifetime spectroscopy (PALS) results

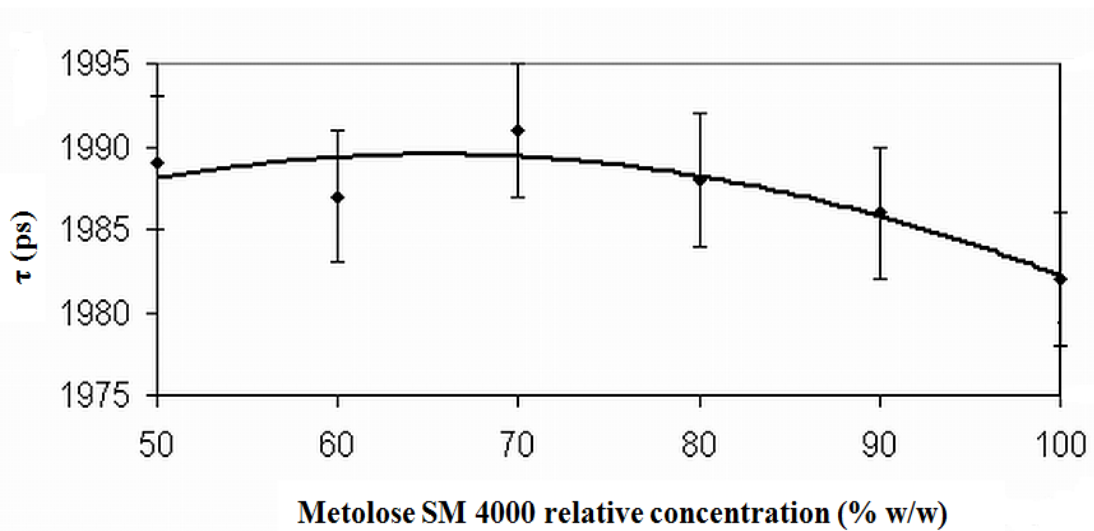
PALS spectroscopy data (Figure 19) showed that the o-Ps distributions are shifted towards higher lifetimes in patches, which contain greater amount of Metolose 90 SH 100.000 SR. However, there is no significant difference between the free volume sizes of the different compositions. The microscopic and macroscopic porosity in the different patches increased with the increased amount of Metolose 90 SH 100.000 SR, which leads to increased permeability, thus resulting in faster initial rate and higher extent of drug release [121, 122].

Figure 21 represents the effect of Metolose SM 4000 relative concentrations on the amount of metoprolol tartrate released at the 6. hour. Along with the increase of the hydroxypropoxy substitution of patches (Metolose 90 SH 100.000 SR), the extent of drug release also increases. The Metolose structure containing hydroxypropoxyl groups enables the formation of H-bonds which initiates the water penetration through the

patches. The expanded swelling increases the size of free volume holes in the film and that, consequently, increases the rate and extent of drug release. As it is obvious from Figures 21 and 22, the drug release properties and the free volume of the films change similarly.



**Figure 21** - Metoprolol tartrate released (% w/w) at the 6. hour as a function of the Metolose SM 4000 relative concentration



**Figure 22** – Ortho-positronium lifetime values of metoprolol tartrate patches as a function of the Metolose SM 4000 relative concentration

The released amount of metoprolol tartrate at the 6. hour (% w/w) and ortho-positronium lifetime ( $\tau$ , ps) values could be described with the following polynomial equation as a function of the relative concentration of Metolose SM 4000 (% w/w) in the patches containing 2% w/w Metolose polymers:

$$y = ax^2 + bx + c \quad (11)$$

where a, b, c are constants. The fitted polynomial curves are shown in both Figure 21 and 22, respectively.

The constants of the polynomial curve were the following in the case of the released metoprolol tartrate vs. Metolose SM 4000:

$$a = -0.00296$$

$$b = 3.3729$$

$$c = 18.295$$

$$R^2 = 0.9857$$

In the case of the ortho-positronium lifetime values vs. Metolose SM 4000, the constants were the following:

$$a = -0.00061$$

$$b = 0.7936$$

$$c = 1963.6$$

$$R^2 = 0.8981$$

The effect of the relative concentration of the Metolose SM 4000 in the patches on the free volume of the polymeric matrix and on the released metoprolol tartrate at the 6. hour can be characterized by a polynomial relationship with good correlation. This relationship helps to design therapeutic systems of predicted drug release.

Although positronium lifetime data do not indicate a dramatic free volume change, their correlation with the drug release properties of the films is obvious. This indicates a very

slightly different structure for films containing metoprolol tartrate depending on their Metolose SM 4000 and Metolose 90 SH 100.000 SR ratio. To clear this problem, the same films without metoprolol tartrate were also studied. Figure 23 represents the o-Ps lifetime values of patches as a function of the Metolose SM 4000 relative concentration.

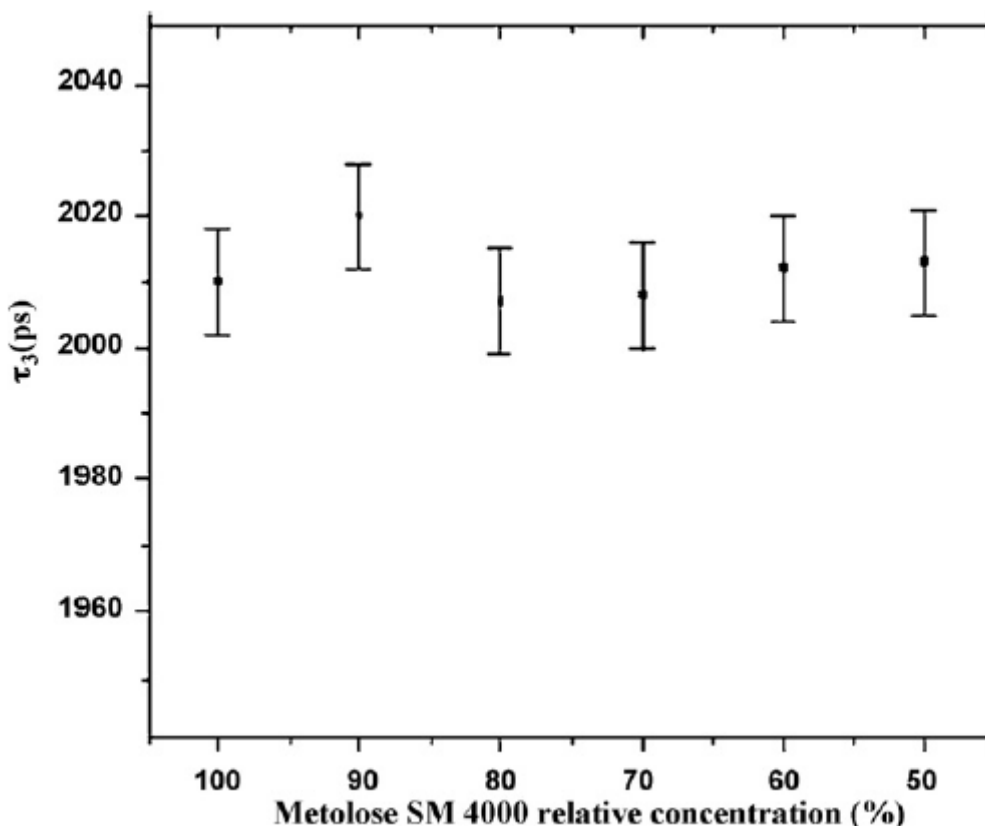


**Figure 23** – Ortho-positronium lifetime values of patches as a function of the Metolose SM 4000 relative concentration

In this case, all of the films were identical from the viewpoint of positron lifetime spectroscopy. All produced the same lifetime of 2010 ps within the statistical error, i.e., all of the films had the same free volume size. This indicates that Metolose SM 4000 and Metolose 90 SH 100.000 SR are interchangeable and have a very similar structure. However, the drug encapsulated in them might react differently for the two variants of Metolose. In the case of metoprolol tartrate as a drug, Metolose 90 SH 100.000 SR provides a faster and a more complete release than Metolose SM 4000.

## **6. NEW SCIENTIFIC RESULTS AND CONCLUSIONS**

New scientific results of the research work:

- Eudragit and Metolose based patches containing metoprolol tartrate were created with different ratios of the applied polymers to evaluate the drug liberation from the different compositions.
- As a result of the pre-formulation work, I determined which polymers from the different types of Eudragit and Metolose enable the formation of TTS patches containing metoprolol tartrate. The combination of Eudragit NE 30 D and different Metolose polymers resulted in novel composition which enabled the formation of TTS patches.
- The supramolecular structural elements, connected via H-bonds, strongly influenced the drug release from the patches. The changes of the supramolecular structure were sensitively tracked with positron annihilation lifetime spectroscopy. The latter enabled the visualization of the free volume changes as a function of the polymer composition.
- The different ratio of Metolose SM 4000 and Metolose 90 SH 100.000 SR could sensitively control the release extent and kinetics of metoprolol tartrate from the patches.
- Eudragit NE 30 D enables the barrier function of the polymer composite, while the drug release profile was controlled by the various proportions of water-soluble Metolose SM 4000 and Metolose 90 SH 100.000 SR.
- The effect of the relative concentration of the Metolose SM 4000 in the patches on the free volume of the polymeric matrix and on the released metoprolol tartrate after the 6. hour can be characterized by a polynomial relationship with good correlation.

- FT-IR spectroscopy was successfully applied as a quick non-destructive method to monitor the stability of intact patches in the course of storage.
- Linear relationship was found with good correlation between the area under the peak measured within the characteristic wavenumber range of the FT-IR curves of Metolose containing patches and the  $\log \tau_{63.2}$  values of metoprolol tartrate release. The application of FT-IR method enables the fast non-invasive in process control of patches of required drug release profile.

## 7. SUMMARY

Metoprolol tartrate is a widely used drug as a beta-blocking agent. The oral administration of this drug leads to intensive first-pass metabolism, it has a short biological half-life and has a bioavailability of 40- to 50%. Among these it has an appropriate skin penetration potential. Due to these characteristics it needs to be frequently dosed and indicates the application of this drug via transdermal route.

These long-acting sustained and controlled release transdermal preparations are able to ensure systemic effect with predetermined time with steady-state delivery rate. They enhance the patient compliance, which is also an important factor of their application.

The purpose of my thesis was to prepare and evaluate matrix type patches containing metoprolol tartrate with different polymer compositions. For this purpose an acrylic polymer (Eudragit NE 30 D) and two types of modified cellulose (Metolose SM 4000 and Metolose 90 SH 100.000 SR) were chosen. The patches were prepared with casting method, which enables a fully homogenized embedding of metoprolol tartrate in the different polymer matrices. The viscosity, the drug release parameters, the FT-IR spectra and the positron annihilation lifetime of the samples were analyzed. The drug release from the patches was tested by the rotating paddle method and the drug release data were analyzed assuming Weibull kinetic model. The hydrophilic behavior of the cellulose polymers and their ratio in the patches can affect the kinetic and the total amount of released drug from the samples. The free volume size changes referred to the microstructural changes of patches depending on the polymer composition, thus the changes in the drug release profile could be confirmed by the o-positronium lifetime changes. The correlation between the FT-IR transmittance characteristics of the patches and the kinetic parameter values of the metoprolol tartrate release ( $\tau_{63.2}$ ) of patches containing Metolose polymers may enable FT-IR measurements as a useful non-destructive means during the in-process control of patches.



## 8. ÖSSZEFOGLALÓ

A metoprolol-tartarát széles körben alkalmazott  $\beta$ -blokkoló hatóanyag, amely adagolása során intenzív first pass metabolizmuson megy keresztül. A farmakon biológiai felezési ideje viszonylag rövid, biohasznosíthatósága 40- és 50% között mozog. Mindezen tulajdonságok mellett megfelelő bőr-penetrációs képességgel rendelkezik. Fentiek alapján elmondható, hogy a metoprolol-tartarát terápiás hatásának eléréséhez a farmakon gyakori adagolása vagy retard készítmény alkalmazása szükséges, amely indokoltá teszi transzdermális készítmény formulálását.

A kontrollált hatóanyag-felszabadulást hosszú ideig biztosító transzdermális készítmények alkalmasak szisztémás hatás kifejtésére előre meghatározott ideig konstans hatóanyag-leadási sebesség mellett. Mindezekon felül alkalmazásuk egyik fontos pozitív tulajdonsága, hogy növelik a betegek terápiás együttműködő-képességét. Értekezésem célja különböző polimerekből álló, metoprolol-tartarát tartalmú tapaszok előállításának és vizsgálata volt. A mátrix előállításához Eudragit NE 30 D és két, módosított cellulózzármazék (Metolose SM 4000 és Metolose 90 SH 100.000 SR) került felhasználásra. A tapaszokat oldatokból öntéses módszerrel állítottam elő. Az oldószer elpárologtatása után a különböző polimer mátrixok a metoprolol-tartarátot teljesen homogén eloszlásban tartalmazták. A tapaszok előállítása során kialakuló reológiai viszonyokat, a hatóanyag-felszabadulás profilját és kinetikai paramétereit elemeztem. A minták mikro- és makroszerkezetének összehasonlítására FT-IR spektroszkópiai és pozitron annihilációs élettartam spektroszkópiai vizsgálatokat végeztem. A minták *in vitro* hatóanyag-felszabadulását forgólapátos módszerrel vizsgáltam, a hatóanyag-felszabadulás kinetikáját pedig Weibull matematikai modell segítségével jellemeztem. A cellulóz polimerek hidrofilitása, illetve azok aránya a mátrixokban befolyásolta a hatóanyag-felszabadulás mennyiségét és kinetikáját. A pozitron élettartam-eloszlás görbék jól szemléltetik a szabadtérfogat változását a különböző polimer arányok függvényében, amely a mikroszerkezet-változást alátámasztja, és a hatóanyag-felszabadulás polimer-szerkezettől függő profiljának magyarázatát adja. A tapaszokat jellemző FT-IR transzmittancia értékek, illetve a metoprolol-tartarát felszabadulását jellemző kinetikai paraméter ( $\tau_{63,2}$ ) értékek között tapasztalható korreláció lehetővé teszi nem-destruktív in-process kontroll alkalmazását.

## 9. REFERENCES

1. RÁCZ, I, SELMECZI, B. Gyógyszertechnológia 1. Gyógyszerformulálás. Budapest: Medicina. 2001:565-575.
2. Shah, VP, Skelly, JP. Regulatory aspects pertinent to the development of transdermal drug delivery systems. Clin Res Pract Drug Regul Aff. 1986;4:433-444.
3. Barry, BW, Bennett, SL. Effect of penetration enhancers on the permeation of mannitol, hydrocortisone and progesterone through human skin. J Pharm Pharmacol. 1987;39:535-546.
4. Whitehead, MI, Fraser, D, Schenkel, L, Crook, D, Stevenson, JC. Transdermal administration of estrogen/progestogen hormone replacement therapy. Lancet. 1990;335:310-312.
5. Ridout, G, Santus, GC, Guy, RH. Pharmacokinetic considerations in the use of newer transdermal formulations. Clin Pharmacokinet. 1988;15:114-131.
6. Shah, VP, Behl, CR, Flynn, GL, Higuchi, WI, Schaefer, H. Principles and criteria in the development and optimization of topical therapeutic products. Pharm Res. 1992;9:1107-1112.
7. Kawahara, K, Tojo, K. Skin irritation in transdermal drug delivery systems: A strategy for its reduction. Pharm Res. 2007;24:399-408.
8. Conjeevaram, R, Chaturvedula, A, Betageri, GV, Sunkara, G, Banga, AK. Iontophoretic in vivo transdermal delivery of beta-blockers in hairless rats and reduced skin irritation by liposomal formulation. Pharm Res. 2003;20:1496-1501.

9. Jibry, N, Murdan, S. In vivo investigation, in mice and in man, into the irritation potential of novel amphiphilic gels being studied as transdermal drug carriers. *Eur J Pharm Biopharm.* 2004;58:107-119.
10. Monkhouse, DC, Huq, AS. Transdermal drug delivery - problems and promises. *Drug Dev Ind Pharm.* 1988;14:183-209.
11. Flynn, GL. Topical drug absorption and topical pharmaceutical systems. In: Benker, GS, Rhode, CT (eds.): *Modern pharmaceuticals.* New York: Dekker. 1979:263-327.
12. Gao, S, Singh, J. Mechanism of transdermal transport of 5-fluorouracil by terpenes: carvone, 1,8-cineole, and thymol. *Int J Pharm.* 1997;154:67-77.
13. Elias, PM. Epidermal lipids, barrier function, and desquamation. *J Invest Dermatol.* 1983;80:44-49.
14. Nowak, GA. *Die kosmetischen Präparate. Rezeptur, Herstellung und wissenschaftliche Grundlagen.* Augsburg: Verlag für chem. Industrie H Ziolkowsky. 1969:1-32.
15. Lin, RY, Chen, WY, Liao, CW. Entropy-driven binding/partition of amino acids/dipeptides to stratum corneum lipid vesicles. *J Controlled Release.* 1998;50:51-59.
16. Lee, RD, White, HS, Scott, ER. Visualization of iontophoretic transport paths in cultured and animal skin models. *J Pharm Sci.* 1996;85:1186-1190.
17. Flynn, GL, Yalkowsky, SH. Correlation and prediction of mass transport across membranes. I. Influence of alkyl chain length on flux-determining properties of barrier and diffusant. *J Pharm Sci.* 1972;61:838-851.

18. Scheuplein, RJ. Mechanism of percutaneous absorption. II. Transient diffusion and the relative importance of various routes of skin penetration. *J Invest Dermatol.* 1967;48:79-88.
19. Scheuplein, RJ, Blank, IH. Permeability of the skin. *Physiol Rev.* 1971;51:702-747.
20. Chen, HB, Zhu, HD, Zheng, JN, Mou, DS, Wan, JL, Zhang, JY, Shi, TL, Zhao YJ, Xu, HB, Yang, XL. Iontophoresis-driven penetration of nanovesicles through microneedle-induced skin microchannels for enhancing transdermal delivery of insulin. *J Controlled Release.* 2009;139:63-72.
21. Wang, YP, Thakur, R, Fan, QX, Michniak, B. Transdermal iontophoresis: combination strategies to improve transdermal iontophoretic drug delivery. *Eur J Pharm Biopharm.* 2005;60:179-191.
22. Vuleta, G, Stupar, M. Influence of decorative cosmetics on the physiological pH of the skin. *Farm Vestn.* 1984;35:19-21.
23. Renner, UD, Oertel, R, Kirch, W. Pharmacokinetics and pharmacodynamics in clinical use of scopolamine. *Ther Drug Monit.* 2005;27:655-665.
24. Donnelly, RF, Singh, TR, Woolfson, AD. Microneedle-based drug delivery systems: microfabrication, drug delivery, and safety. *Drug Deliv.* 2010;17:187-207.
25. Ceschel, GC, Maffei, P, Borgia, SL. Correlation between the transdermal permeation of ketoprofen and its solubility in mixtures of a pH 6.5 phosphate buffer and various solvents. *Drug Deliv.* 2002;9:39-45.
26. Kubota, K, Koyama, E, Yasuda, K. Random walk method for percutaneous drug absorption pharmacokinetics: application to repeated administration of a

therapeutic timolol patch. *J Pharm Sci.* 1991;80:752-756.

27. Wang, MY, Yang, YY, Heng, PW. Skin permeation of physostigmine from fatty acids-based formulations: evaluating the choice of solvent. *Int J Pharm.* 2005;290:25-36.
28. Pfister, WR. Transdermal and dermal therapeutic systems: current status. In: Ghosh, TK, Pfister, WR, and Yum, SI (eds.): *Transdermal and topical drug delivery systems.* Buffalo Grove: Interpharm Press. 1997:33–112.
29. Foreman, MI. Stratum corneum hydration: consequences for skin permeation experiments. *Drug Dev Ind Pharm.* 1986;12:461-463.
30. Tronnier, H. Hydration of the skin. *J Soc Cosmet Chem.* 1981;32:175-192.
31. Masada, T, Higuchi, WI, Srinivasan, V, Rohr, U, Pons, S, Fox, J. Examination of iontophoretic transport of ionic drugs across skin: baseline studies with the four-electrode system. *Int J Pharm.* 1989;49:57-62.
32. Paudel, KS, Hammell, DC, Agu, RU, Valiveti, S, Stinchcomb, AL. Cannabidiol bioavailability after nasal and transdermal application: effect of permeation enhancers. *Drug Dev Ind Pharm.* 2010;36:1088-1097.
33. El-Laithy, HM. Novel transdermal delivery of timolol maleate using sugar esters: preclinical and clinical studies. *Eur J Pharm Biopharm.* 2009;72:239-245.
34. Ben-Shabat, S, Baruch, N, Sintov, AC. Conjugates of unsaturated fatty acids with propylene glycol as potentially less-irritant skin penetration enhancers. *Drug Dev Ind Pharm.* 2007;33:1169-1175.
35. Zhou, Y, Wei, YH, Zhang, GQ, Wu, XA. Synergistic penetration of ethosomes and lipophilic prodrug on the transdermal delivery of acyclovir. *Arch Pharm Res.*

2010;33:567-574.

36. Kiptoo, PK, Paudel, KS, Hammell, DC, Pinninti, RR, Chen, J, Crooks, PA, Stinchcomb, AL. Transdermal delivery of bupropion and its active metabolite, hydroxybupropion: A prodrug strategy as an alternative approach. *J Pharm Sci.* 2009;98:583-594.
37. Akomeah, FK, Martin, GP, Brown, MB. Short-term iontophoretic and post-iontophoretic transport of model penetrants across excised human epidermis. *Int J Pharm.* 2009;367:162-168.
38. Denet, AR, Ucakar, B, Preat, V. Transdermal delivery of timolol and atenolol using electroporation and iontophoresis in combination: A mechanistic approach. *Pharm Res.* 2003;20:1946-1951.
39. Abla, N, Naik, A, Guy, RH, Kalia, YN. Effect of charge and molecular weight on transdermal peptide delivery by iontophoresis. *Pharm Res.* 2005;22:2069-2078.
40. Pillai, O, Nair, V, Panchagnula, R. Transdermal iontophoresis of insulin: IV. Influence of chemical enhancers. *Int J Pharm.* 2004;269:109-120.
41. Tokumoto, S, Higo, N, Sugibayashi, K. Effect of electroporation and pH on the iontophoretic transdermal delivery of human insulin. *Int J Pharm.* 2006;326:13-19.
42. Brown, MB, Martin, GP, Jones, SA, Akomeah, FK. Dermal and transdermal drug delivery systems: Current and future prospects. *Drug Deliv.* 2006;13:175-187.
43. Murthy, SN, Sen, A, Hui, SW. Surfactant-enhanced transdermal delivery by electroporation. *J Controlled Release.* 2004;98:307-315.

44. Rao, R, Nanda, S. Sonophoresis: recent advancements and future trends. *J Pharm Pharmacol.* 2009;61:689-705.
45. Yang, JH, Kim, DK, Yun, MY, Kim, TY, Shin, SC. Transdermal delivery system of triamcinolone acetonide from a gel using phonophoresis. *Arch Pharm Res.* 2006;29:412-417.
46. Machet, L, Boucaud, A. Phonophoresis: efficiency, mechanisms and skin tolerance. *Int J Pharm.* 2002;243:1-15.
47. Escobar-Chavez, JJ, Quintanar-Guerrero, D, Ganem-Quintanar, A. In vivo skin permeation of sodium naproxen formulated in pluronic F-127 gels: Effect of Azone(R) and Transcutol(R). *Drug Dev Ind Pharm.* 2005;31:447-454.
48. Csóka, G, Pásztor, E, Marton, S, Zelkó, R, Antal, I, Klebovich, I. Formulation of thermoresponsive transdermal therapeutic systems using cellulose derivatives. *Acta Pharm Hung.* 2007;77:102-107.
49. Csóka, G, Gelencsér, A, Makó, A, Marton, S, Zelkó, R, Klebovich, I, Antal, I. Potential application of Metolose(R) in a thermoresponsive transdermal therapeutic system. *Int J Pharm.* 2007;338:15-20.
50. Djedour, A, Boury, F, Grossiord, JL. Modulation of the release from a w/o/w multiple emulsion by controlling the viscoelastic properties of the two interfaces. *J Drug Deliv Sci Technol.* 2009;19:197-203.
51. Jones, DS, Bruschi, ML, de Freitas, O, Gremiao, MP, Lara, EH, Andrews, GP. Rheological, mechanical and mucoadhesive properties of thermoresponsive, bioadhesive binary mixtures composed of poloxamer 407 and carbopol 974P designed as platforms for implantable drug delivery systems for use in the oral cavity. *Int J Pharm.* 2009;372:49-58.

52. Atyabi, F, Khodaverdi, E, Dinarvand, R. Temperature modulated drug permeation through liquid crystal embedded cellulose membranes. *Int J Pharm.* 2007;339:213-221.
53. Moss, J, Bundgaard, H. Prodrugs of peptides. Part 7. Transdermal delivery of thyrotropin-releasing hormone (TRH) via prodrugs. *Int J Pharm.* 1990;66:39-45.
54. Friend, D, Catz, P, Heller, J, Reid, J, Baker, R. Transdermal delivery of levonorgestrel. Part 2. Effect of prodrug structure on skin permeability in vitro. *J Controlled Release.* 1988;7:251-261.
55. Morris, AP, Brain, KR, Heard, CM. Skin permeation and ex vivo skin metabolism of O-acyl haloperidol ester prodrugs. *Int J Pharm.* 2009;367:44-50.
56. Yamada, K, Tojo, K. Bioconversion of estradiol esters in the skin of various animal models in vitro. *Eur J Pharm Biopharm.* 1997;43:253-258.
57. Tojo, K, Valia, KH, Chotani, G, Chien, YW. Long term permeation kinetics of estradiol. Part 4. Theoretical approach to the simultaneous skin permeation and bioconversion of estradiol esters. *Drug Dev Ind Pharm.* 1985;11:1175-1193.
58. Valia, KH, Tojo, K, Chien, YW. Long term permeation kinetics of estradiol. Part 3. Kinetic analyses of the simultaneous skin permeation and bioconversion of estradiol esters. *Drug Dev Ind Pharm.* 1985;11:1133-1173.
59. Ghosh, TK, Banga, AK. Methods of enhancement of transdermal drug delivery: Part 2B. Chemical permeation enhancers. *Pharm Technol.* 1993;17:68, 70-72, 74, 76.
60. Finnin, BC, Morgan, TM. Transdermal penetration enhancers: applications, limitations, and potential. *J Pharm Sci.* 1999;88:955-958.



61. Bodde, HE, Verhoeven, J, van Driel, LM. The skin compliance of transdermal drug delivery systems. *Crit Rev Ther Drug Carrier Syst.* 1989;6:87-115.
62. Seki, T, Kawaguchi, T, Sugibayashi, K, Juni, K, Morimoto, Y. Percutaneous absorption of azidothymidine in rats. *Int J Pharm.* 1989;57:73-75.
63. Larrucea, E, Arellano, A, Santoyo, S, Ygartua, P. Combined effect of oleic acid and propylene glycol on the percutaneous penetration of tenoxicam and its retention in the skin. *Eur J Pharm Biopharm.* 2001;52:113-119.
64. Loftsson, T, Gudmundsdottir, TK, Fridriksdottir, H, Sigurdardottir, AM, Thorkelsson, J, Gudmundsson G, Hjaltason, B. Fatty acids from cod liver oil as skin penetration enhancers. *Pharmazie.* 1995;50:188-190.
65. Seki, T, Morimoto, K. Enhancing effects of medium chain aliphatic alcohols and esters on the permeation of 6-carboxyfluorescein and indomethacin through rat skin. *Drug Deliv.* 2003;10:289-293.
66. Anigbogu, AN, Williams, AC, Barry, BW, Edwards, HG. Fourier transform Raman spectroscopy of interactions between the penetration enhancer dimethyl sulfoxide and human stratum corneum. *Int J Pharm.* 1995;125:265-282.
67. Hwang, CC, Danti, AG. Percutaneous absorption of flufenamic acid in rabbits: effect of dimethyl sulfoxide and various nonionic surface active agents. *J Pharm Sci.* 1983;72:857-860.
68. Thacharodi, D, Panduranga Rao, K. Collagen membrane controlled transdermal delivery of propranolol hydrochloride. *Int J Pharm.* 1996;131:97-99.
69. Csóka, G, Marton, S, Zelkó, R, Otomo, N, Antal, I. Application of sucrose fatty acid esters in transdermal therapeutic systems. *Eur J Pharm Biopharm.* 2007;65:233-237.

70. Murthy, TE, Kishore, VS. Effect of casting solvent and polymer on permeability of propranolol hydrochloride through membrane controlled transdermal drug delivery system. *Indian J Pharm Sci.* 2007;69:646-650.
71. Misra, A, Pal, R, Majumdar, SS, Talwar, GP, Singh, O. Biphasic testosterone delivery profile observed with two different transdermal formulations. *Pharm Res.* 1997;14:1264-1268.
72. Ghosh, TK, Habib, MJ, Childs, K, Alexander, M. Transdermal delivery of metoprolol. Part 1. Comparison between hairless mouse and human cadaver skin and effect of n-decylmethyl sulfoxide. *Int J Pharm.* 1992;88:391-396.
73. Ghosh, TK, Bagherian, A. Development of a transdermal patch of methadone: in vitro evaluation across hairless mouse and human cadaver skin. *Pharm Dev Technol.* 1996;1:285-291.
74. Venkatesh, S, Hodgkin, L, Hanson, P, Suryanarayanan, R. In vitro release kinetics of salicylic acid from hydrogel patch formulations. *J Controlled Release.* 1992;18:13-18.
75. Jain, SK, Vyas, SP, Dixit, VK. Effective and controlled transdermal delivery of ephedrine. *J Controlled Release.* 1990;12:257-263.
76. Costa, P, Ferreira, DC, Morgado, R, Sousa Lobo, JM. Design and evaluation of a lorazepam transdermal delivery system. *Drug Dev Ind Pharm.* 1997;23:939-944.
77. Livingstone, C, Livingstone, D. Drug delivery. Part 1. Transdermal systems. *Pharm J.* 1988;241:130-131.
78. Rácz, I. *Drug Formulation.* Budapest: Medicina. 1984:327-342.
79. Higuchi, T. Physical chemical analysis of percutaneous absorption process from creams and ointments. *J Soc Cosmet Chem.* 1960;11:85-97.

80. Roy, SD, Gutierrez, M, Flynn, GL, Cleary, GW. Controlled transdermal delivery of fentanyl: characterization of pressure-sensitive adhesives for matrix patch design. *J Pharm Sci.* 1996;85:491-495.
81. Morimoto, Y, Kokubo, T, Sugibayashi, K. Diffusion of drugs in acrylic-type pressure-sensitive adhesive matrix. Part 2. Influence of interaction. *J Controlled Release.* 1992;18:113-121.
82. Higuchi, T. Mechanism of sustained-action medication. *J Pharm Sci.* 1963;52:1145-1147.
83. Higuchi, T. Rate of release of medicaments from ointment bases containing drugs in suspension. *J Pharm Sci.* 1961;50:874-875.
84. Desai, SJ, Simonelli, AP, Higuchi, WI. Investigation of factors influencing release of solid drug dispersed in inert matrices. *J Pharm Sci.* 1965;54:1459-1464.
85. Desai, SJ, Singh, P, Simonelli, AP, Higuchi, WI. Investigation of factors influencing release of solid drug dispersed in inert matrices II. *J Pharm Sci.* 1966;55:1224-1229.
86. Dredán, J, Antal, I, Rácz, I. Evaluation of mathematical models describing drug release from lipophilic matrices. *Int J Pharm.* 1996;145:61-64.
87. Su, XY, Al-Kassas, R, Li Wan Po, A. Statistical modelling of ibuprofen release from spherical lipophilic matrices. *Eur J Pharm Biopharm.* 1994;40:73-76.
88. Langenbucher, F. Parametric representation of dissolution rate curves by the RRSBW distribution. *Pharm Ind.* 1976;38:474-477.

89. Regardh, CG, Borg, KO, Johansson, R, Johansson, G, Palmer, L. Pharmacokinetic studies on the selective beta1-receptor antagonist metoprolol in man. *J Pharmacokinet Biopharm.* 1974;2:347-364.
90. Yuen, KH, Peh, KK, Chan, KL, Toh, WT. Pharmacokinetic and bioequivalent study of a generic metoprolol tablet preparation. *Drug Dev Ind Pharm.* 1998;24:955-959.
91. Kommuru, TR, Khan, MA, Reddy, IK. Effect of chiral enhancers on the permeability of optically active and racemic metoprolol across hairless mouse skin. *Chirality.* 1999;11:536-540.
92. Bhatt, DC, Dhake, AS, Khar, RK, Mishra, DN. Development and in vitro evaluation of transdermal matrix films of metoprolol tartrate. *Yakugaku Zasshi.* 2008;128:1325-1331.
93. European Pharmacopoeia 6th Edition. Strasbourg (France): Council of Europe. 2010.
94. Rowe, CR, Sheskey, PJ, Quinn, ME. Handbook of Pharmaceutical Excipients 6th Edition. London: Pharmaceutical Press. 2009:524-533, 438, 326-329.
95. <http://www.elementoorganika.ru/files/metolose.pdf> [cited 2011.09.17.]
96. Wan, LS, Prasad, KP. Uptake of water by excipients in tablets. *Int J Pharm.* 1989;50:147-153.
97. Esezobo, S. Disintegrants: effects of interacting variables on the tensile strengths and dissolution times of sulfoguanidine tablets. *Int J Pharm.* 1989;56:207-211.
98. Wan, LS, Lai, WF. Factors affecting drug release from drug-coated granules prepared by fluidized-bed coating. *Int J Pharm.* 1991;72:163-174.

99. Dalal, PS, Narurkar, MM. In vitro and in vivo evaluation of sustained release suspensions of ibuprofen. *Int J Pharm.* 1991;73:157-162.
100. Sultana, Y, Aqil, M, Ali, A, Zafar, S. Evaluation of carbopol-methyl cellulose based sustained-release ocular delivery system for pefloxacin mesylate using rabbit eye model. *Pharm Dev Technol.* 2006;11:313-319.
101. Chowhan, ZT. Role of binders in moisture induced hardness increase in compressed tablets and its effect on in vitro disintegration and dissolution. *J Pharm Sci.* 1980;69:1-4.
102. Rowe, RC. The molecular weight and molecular weight distribution of hydroxypropyl methylcellulose used in the film coating of tablets. *J Pharm Pharmacol.* 1980;32:116-119.
103. Okhamafe, AO, York, P. Characterization of moisture interactions in some aqueous based tablet film coating formulations. *J Pharm Pharmacol.* 1985;37:385-390.
104. Wilson, HC, Cuff, GW. Sustained release of isomazole from matrix tablets administered to dogs. *J Pharm Sci.* 1989;78:582-584.
105. Barakat, NS, Omar, SA, Ahmed, AA. Carbamazepine uptake into rat brain following intra-olfactory transport. *J Pharm Pharmacol.* 2006;58:63-72.
106. Eldrup, M, Lightbody, D, Sherwood, JN. The temperature dependence of positron lifetimes in solid pivalic acid. *Chem Phys.* 1981;63:51-58.
107. Szente, V, Süvegh, K, Marek, T, Zelkó, R. Prediction of the stability of polymeric matrix tablets containing famotidine from the positron annihilation lifetime distributions of their physical mixtures. *J Pharm Biomed Anal.* 2009;49:711-714.

108. Süvegh, K, Zelkó, R. Physical ageing of polyvinylpyrrolidone under different humidity conditions. *Macromolecules*. 2002;35:795-800.
109. <http://eudragit.evonik.com/sites/dc/Downloadcenter/Evonik/Product/EUDRAGIT/EUDRAGIT%20Products.pdf> [cited 2011.09.15.]
110. Madishetti, SK, Palem, CR, Gannu, R, Thatipamula, RP, , Panakanti, PK, Yamsani, MR. Development of domperidone bilayered matrix type transdermal patches: physicochemical, in vitro and ex vivo characterization. *Daru*. 2010;18:221-229.
111. Mamatha, T, Rao, JV, Mukkanti, K, Ramesh, G. Formulation and in vitro evaluation of transdermal patches of lercanidipine hydrochloride. *Acta Pharm Turc*. 2010;52:295-304.
112. Mamatha, T, Rao, JV, Mukkanti, K, Ramesh, G. Development of matrix type transdermal patches of lercanidipine hydrochloride: physicochemical and in-vitro characterization. *Daru*. 2010;18:9-16.
113. El-Gendy, NA, Sabry, NA, El-Attar, M, Omar, E, Mahmoud, M. Transdermal delivery of salbutamol sulphate: Formulation and evaluation. *Pharm Dev Technol*. 2009;14:216-225.
114. Tanwar, YS, Chauhan, CS, Sharma, A. Development and evaluation of carvedilol transdermal patches. *Acta Pharm*. 2007;57:151-159.
115. Valenta, C, Biebel, R. In vitro release study of transdermal delivery systems of progesterone. *Drug Dev Ind Pharm*. 1998;24:187-191.
116. Valenta, C, Almasi-Szabo, I. In vitro diffusion studies of ketoprofen transdermal therapeutic systems. *Drug Dev Ind Pharm*. 1995;21:1799-1805.

117. Aqil, M, Sultana, Y, Ali, A. Matrix type transdermal drug delivery systems of metoprolol tartrate: *In vitro* characterization. *Acta Pharm.* 2003;53:119-125.
118. Florey, K. Analytical profiles of drug substances. Vol. 12. New York: Academic Press. 1983:342-343.
119. Bright, A, Renuga Devi, TS, Gunasekaran, S. Spectroscopical vibrational band assignment and qualitative analysis of biomedical compounds with cardiovascular activity. *Int J Chem Tech Res.* 2010;2: 379-388.
120. Papp, J, Horgos, J, Szente, V, Zelkó, R. Correlation between the FT-IR characteristics and metoprolol tartrate release of methylcellulose-based patches. *Int J Pharm.* 2010;392:189-191.
121. Papp, J, Szente, V, Süvegh, K, Zelkó, R. Correlation between the free volume and the metoprolol tartrate release of Metolose patches. *J Pharm Biomed Anal.* 2010;51:244-247.
122. Papp, J, Marton, S, Süvegh, K, Zelkó, R. The influence of Metolose structure on the free volume and the consequent metoprolol tartrate release of patches. *Int J Biol Macromol.* 2009;44:6-8.

## 10. PUBLICATIONS AND LECTURES

### Publications

**Papp, J**, Horgos, J, Szente, V, Zelkó, R. Correlation between the FT-IR characteristics and metoprolol tartrate release of methylcellulose-based patches. *Int J Pharm.* 2010;392:189-191. IF= 3,607

**Papp, J**, Szente, V, Süvegh, K, Zelkó, R. Correlation between the free volume and the metoprolol tartrate release of Metolose patches. *J Pharm Biomed Anal.* 2010;51:244-247. IF=2,733

**Papp, J**, Marton, S, Süvegh, K, Zelkó, R. The influence of Metolose structure on the free volume and the consequent metoprolol tartrate release of patches. *Int J Biol Macromol.* 2009;44:6-8. IF=2,366

### Book chapter

**Papp, J**, Zelkó, R. Significance of the nonionic surfactants – A pharmaceutical approach. In: Wendt, PL, Hoysted DS (eds.): *Non-Ionic Surfactants*. Hauppauge, NY: Nova Science Publishers Inc. 2009: 229-244.

### Lectures

**Papp, J**, Marton, S, Csóka, G. Eudragit NE 30 D tartalmú membrán kontrollált TTS rendszerek formulálása és vizsgálata. *Congressus Pharmaceuticus Hungaricus XIII.* Budapest, 2006. május 25-27.



## 11. ACKNOWLEDGEMENTS

This thesis was created with the help of my tutor, Professor Sylvia Marton (Department of Pharmaceutics, Semmelweis University). I am greatly thankful for her guiding and supporting with her knowledge. I am also very grateful for providing me the opportunity to work in the institute.

I am greatly indebted to Professor Romána Zelkó for her energy and unselfish support in my thesis. The discussions and collaboration during the work will always stay in my memory.

Furthermore, I express my special thanks to Dr. Gabriella Csóka, whom with I was introduced into the pharmaceutical practice. The participation of Pálné Reimann in my practical work was very inspiring.

I am very thankful to Dr. Károly Süvegh for the PALS analysis. *I am grateful to my parents and family.*